



- 1 Geochemical characteristics of suspended particulate matter around Piscadera Bay and its
- 2 influence on near shore ecosystems, Curação (Caribbean Sea)
- 4 Virginia Sánchez Barranco^{1*}; Nienke C.J. van de Loosdrecht²; Furu Mienis¹; Jasper M. de Goeij²;
- 5 Rick Hennekam¹; Gert-Jan Reichart^{1,3}; Jan-Berend Stuut^{1,4}; Lennart J. de Nooijer¹
- ⁶ Royal Netherlands Institute for Sea Research (NIOZ), department of Ocean Systems, Den
- 7 Burg, The Netherlands.
- 8 ² Institute for Biodiversity and Ecosystem Dynamics (IBED), University van Amsterdam,
- 9 Amsterdam, The Netherlands.
- 10 3 Department of Earth Sciences, Faculty of Geosciences, Utrecht University, Budapestlaan 4,
- 11 3584 CD Utrecht, The Netherlands.
- 12 ⁴ Vrije Universiteit Amsterdam (VU Amsterdam), Amsterdam, The Netherlands.
- 13 *Corresponding author

17

18

19

20 21

22 23

24

25

26

27 28

29

30

31 32 Abstract. Caribbean coral reefs face rising pressure from coastal development, yet the pathways by which urban pollution reaches these endangered ecosystems remain poorly understood. Bays act as dynamic channels, trapping, transforming, and releasing materials that can impact adjacent reef systems. We investigated the seasonal and spatial variability of suspended particulate matter (SPM)—a key vector for pollutants and nutrients— coming from an urbanized bay in Curação and determined its effect on surrounding coral reefs. Using sediment traps deployed across spatial gradients (bay mouth to nearby reefs in the East and West) during the dry (April-May) and wet (October-November) seasons, we measured mass, carbon, and nitrogen fluxes and associated grain-size and geochemical particle composition. Results were compared to environmental conditions (e.g. rain fall, current speed) and revealed a clear spatial gradient of bay influence: the bay mouth showed the strongest terrestrial signal, followed by the eastern reef (sheltered from currents) with elevated SPM fluxes of fine particles enriched in terrigenous elements (Si, Fe, Al, and Mn), while the western reef (exposed to open-ocean flow) exhibited lower fluxes of coarser particles with elevated Ca/Fe, Pb, Cu and Ni. This indicates diminished bay effect and stronger marine influence mixed with localized pollution. During the dry season, differences in SPM fluxes and composition between reef sites were minimal, but wet season conditions amplified spatial patterns, with





rainfall-driven runoff locally increasing dissolved and particular matter delivery. This implies

34 that reef vulnerability to bay-derived pollution locally depends on both proximity to source

waters and seasonal hydrodynamic variability, with sheltered reefs experiencing the greatest

36 impacts during periods of enhanced terrestrial runoff.

37 Key words: SPM, Coral reefs, Terrestrial runoff, Spatial gradient, Seasonal variability, Carbon

38 flux

35

39

40

41 42

43

44

45 46

47 48

49 50

51

52

53

54

55

56

57

58

59

60 61

62

1. Introduction

In recent decades, land-use changes and coastal development around watersheds have increased runoff of sediments, nutrients and chemical pollutants into tropical coastal waters, posing significant threats to coral reefs worldwide, including those in the Caribbean (Burke and Maidens, 2004; Burke et al., 2011). The accumulation of terrestrial discharge on nearshore reefs cause local changes to reef communities, for example the increased cover of (macro)algae (Fabricius, 2005) or suffocation of corals (Weber et al., 2006). Local stressors make them also more vulnerable to global ones, such as thermal bleaching and ocean acidification due to compounded energy deficits and impaired recovery pathways (Storlazzi et al., 2015; Dutra et al., 2018; Anthony et al., 2008). Inland bays on Caribbean islands could play an important role in the supply of sediments, nutrients and pollutants. They show strong environmental variability (diel and seasonal) in physicochemical parameters and higher nutrient and pollutant concentrations compared to reef waters (de Jong et al. 2025), and serve as locations where land-derived substances are retained, transformed, or exported to coastal waters (Heiskanen and Tallberg, 1999). In tropical island environments, discharge from bays is typically episodic, occurring mainly during the rainy season and storm events leading to pulses of material and runoff being released into the ocean (Ringuet and Mackenzie, 2005; De Carlo et al., 2007; Sánchez Barranco et al., 2025; Larson et al., 2015). Suspended particulate matter (SPM) plays a key role in the transport and cycling of minerals,

organic matter, nutrients, and pollutants, all of which can influence coral reef health (Jouon et al., 2008). For example, sediment plumes, often dominated by fine-grained material, can reduce light availability and physically stress coral reefs, especially near river mouths and coastal bays (Fabricius, 2005; Ramos-Scharrón and Macdonald, 2005). Sedimentation from SPM can also physically smother coral polyps, impair recruitment, and increase mortality

https://doi.org/10.5194/egusphere-2025-4873 Preprint. Discussion started: 28 November 2025 © Author(s) 2025. CC BY 4.0 License.



63

64 65

66 67

68

69 70

71

72

73 74

75 76

77 78

79

80

81

82

83

84 85

86

87 88

89 90

91

92

93



(Bhuyan et al., 2025; Erftemeijer et al., 2012). The energetic cost of shedding sediments—via mucus production and ciliary action—can further compromise coral metabolism and resilience (Tuttle and Donahue, 2022). Some studies also show that certain reef organisms can benefit from SPM. For instance, soft corals may utilize detritus and other small SPM (<10 μm particle size) as an important food source, particularly in high-turbidity environments (Anthony, 1999; Fabricius and Dommisse, 2000). De Jong et al. (2025) have shown that the environmental conditions in semi-enclosed bays, where coral communities often persist, can be highly variable compared to open reefs. Reduced light penetration due to suspended sediments limits the photosynthetic energy available for coral growth and reproduction, with finer-grained and darker-coloured sediments causing more pronounced effects than coarser, lighter ones (Anthony and Fabricius, 2000; Weber et al., 2006; Storlazzi et al., 2015). In addition, fine-grained SPM remains longer in suspension, leading to prolonged elevated levels of turbidity. Beyond its impact on light availability, SPM also plays a crucial role in pollutant dynamics. Heavy metals and organic contaminants readily bind to SPM, particularly clays and silts, making them a critical vector for pollutant transport in near-shore marine environments (Salomons and Förstner, 2012; Zhang et al., 2018). This is of particular concern in the Caribbean, where metal pollution poses ecological risks due to its persistence in reef ecosystems (Berry et al., 2013; Guzmán and Jiménez, 1992). The south coast of Curação is characterized by several inland bays that may contribute to the transport of particulate substances to nearby coastal ecosystems, including coral reefs, mangroves, and seagrass beds (Debrot et al., 1998; Wagenaar Hummelinck, 1977). Despite a 50% loss in coral cover over the past 50 years (Sandin et al., 2022) the reefs along the south coast of Curaçao (southeastern Caribbean) are still considered among the healthiest in the Caribbean Sea (Sandin et al., 2008a; Rijsberman and Westmacott, 2000; Sandin et al., 2022; Jackson et al., 2014). Seasonal bay-ocean exchange dynamics are influencing the watercolumn characteristics of nearby coastal ecosystems (Sánchez Barranco et al., 2025). In Curação, bay-ocean exchange is limited during the dry season, leading to the build-up of nutrient concentrations within the bays, whereas during the wet season, increased mixing between bay and offshore waters is enhanced (Sánchez Barranco et al., 2025). These dynamic exchange processes potentially create a complex mechanism for sediment and nutrient transfer between coastal environments. However, while it is known that bays release SPM into





surrounding waters (Restrepo et al., 2016; D'sa and Ko, 2008), the extent of its distribution, 94 deposition, and seasonal variability, and effect on changes in benthic composition, remain 95 96 poorly quantified. Here, we aim to quantify fluxes of SPM and assess their geochemical characteristics in 97 proximity and further away from a bay located on the Caribbean Island Curação. The coastal 98 zone near Piscadera Bay, located on the south coast of Curação, has been studied extensively 99 100 and has one of the longest benthic cover records in the world (De Bakker et al., 2017) providing 101 a unique site to study the potential influence of bay discharge on nearby reefs. We present a 102 study in which sediment traps were deployed for 30 days at various locations around Piscadera 103 Bay during April/May (dry season) and October/November 2023 (wet season). Seasonal 104 variability in SPM fluxes, sampled in the dry and wet seasons, was compared to environmental 105 conditions (e.g. rainfall, wind, tides) to determine if they explain the observed spatio-temporal 106 variability in SPM fluxes and composition. Collected material was analyzed for grain size,

2. Methodology

elemental, and organic matter composition.

2.1 Study site

107

108

109

110

111

112

113114

115

116

117

118

119

120121

122

The island of Curaçao lies near the Venezuelan coast with a surface area of approximately 444 km² and around 150.000 inhabitants and around 1.2 million (cruise) tourists visit the island annually. The south coast is bordered by fringing reefs that start at a water depth of approximately 7 m followed by a steep slope down to 30–50 m (Bak, 1977; De Bakker et al., 2016). The island is characterized by a semi-arid climate, including a wet season with highest precipitation rates in the months of October-December (ranging between 80-115 mm per month) and a dry season with lowest monthly rainfall in April-June (ranging between 8-15 mm per month) (Wit et al., 2025)

This study focuses on Piscadera Bay (Fig. 1), an area that serves as an important catchment area, draining 16–17 km² of the mid-west part of the island of Curaçao (Sánchez Baranco et al., 2025). The bay's wide mouth (ranging from 76 m at its narrowest point to 105 m at its widest) has a shallow entrance of less than 6 m deep. Originally, Piscadera Bay opened to the sea through a narrow, shallow channel, mostly blocked by a coral and debris bar, with a cross-

https://doi.org/10.5194/egusphere-2025-4873 Preprint. Discussion started: 28 November 2025 © Author(s) 2025. CC BY 4.0 License.





sectional area of only 7 m². In 1962, the entrance was widened to 45 m², and in the early 123 124 seventies it was further enlarged and deepened (Hofker, 1971). The reef sites surrounding the bay reflect significant ecological changes over time (Sandin et 125 al., 2022; De Bakker et al., 2017). The reef west of the bay's mouth, which has experienced 126 127 substantial coral degradation, showed 8.2% hard coral cover in 2015, compared to an estimated 40% in 1982, with 29.7% turf cover and 2.7% cyanobacterial mats in 2015 (Sandin 128 et al., 2022; Van Duyl, 1985). The reef directly east of Piscadera's mouth also experienced an 129 ecological transformation, with hard coral cover declining from an estimated 5% in 1982 to 130 merely 0.9% in 2015, accompanied by 51.5% turf cover and 11.5% cyanobacterial mats (De 131 Bakker et al., 2016; Van Duyl, 1985; Sandin et al., 2022) 132 133 Fieldwork was conducted in April-May (dry season) and October-November (wet season) 2023. Sediment traps were deployed for 30 days at the mouth of the bay (3-5 m water depth), 134 135 at the east reef side at 8 and 18 m water depth and at the west reef side of the bay at 8 and 18 m water depth (Fig. 1). At each site, 6 traps were deployed at least 1 m apart from each 136 other following Storlazzi et al. (2011). 137





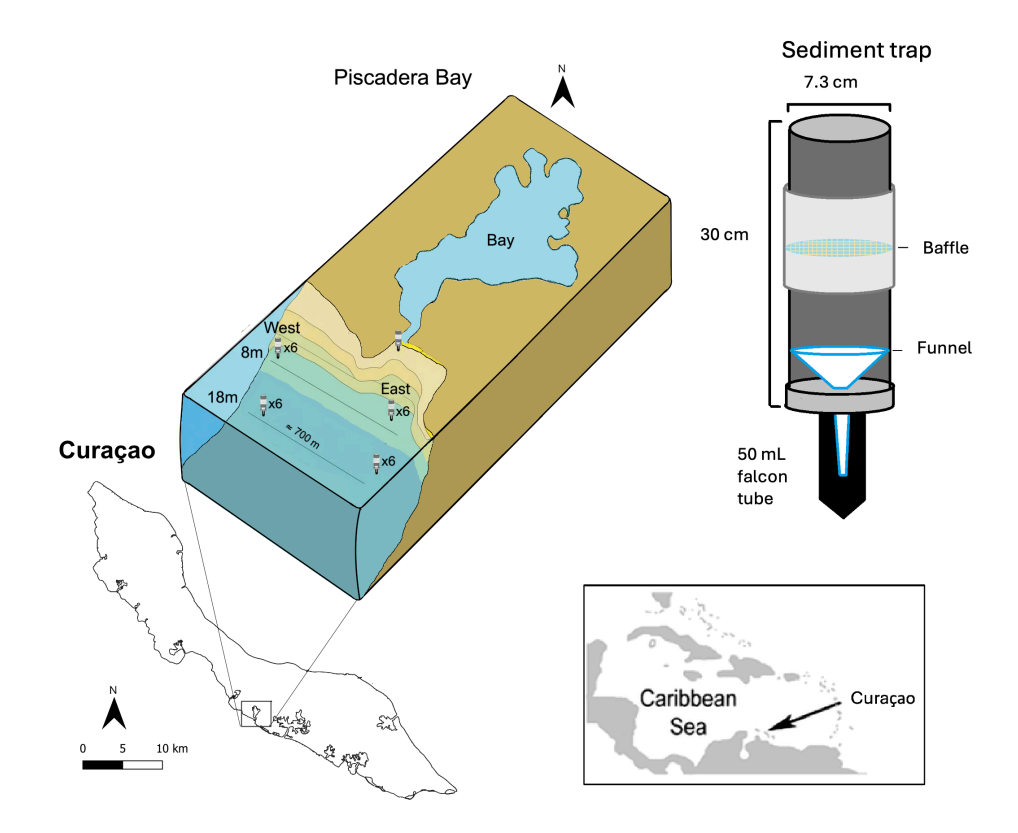


Figure 1. Map of Curaçao showing the studied location of Piscadera Bay on the west side of Willemstad. The inset provides a detailed sketch of the study area around Piscadera Bay, with sediment traps deployed at the bay mouth and at eastern and western reef at depths of 8 m and 18 m. The sediment traps used, follow the design recommendations of Storlazzi et al. (2011) and is shown on the right side for reference.

2.2 Current sensors and environmental data

In October–November 2023, two Acoustic Doppler Current Profilers (ADCP) were deployed at a depth of 10 m at the eastern and western reef of Piscadera Bay for a 30-d period. In April–May 2023, the ADCPs were also deployed for shorter periods of time at the mouth (7 d), eastern (4 d), and western reef (20 d). The ADCPs were used to measure current speed and direction, water temperature, and pressure, which was used to determine tidal cycles. Water speed and direction data used in this study were taken from ADCP bin 3 located 2 m above the seafloor, which corresponded to 8 m water depth at the reef sites (with a total water depth



154155

156

157

158

159160

161

162

163164

165166

167

168169

170171

172

173

174175

176

177

178179

180

181

182



of 10 m) and 3 m water depth near the mouth of the bay (with a total water depth of 5 m). Precipitation and wind data during the sampling periods were retrieved from the Meteorological Department of Curação (Meteorological Department Curação, n.d.).

2.3 Sediment traps and mass fluxes

Sediment traps were built following Storlazzi et al. (2011), with a height of 30 cm, and a surface area of 41.85 cm 2 . Traps (n = 6 per site and depth) were secured with a steel rebar into the sediments with their mouths at 0.7-0.8 m above the seafloor. Inside the trap a baffle was placed to avoid organisms or large objects entering the funnel. At the bottom of the trap, a funnel connected to a 50 mL dark falcon tube was used to collect suspended particulate matter. In April–May 2023, traps at the mouth of the bay were sampled every 5 d and the ones in the eastern and western reef every 10 d. In October-November 2023, Falcon tubes were replaced every 5 d at each location. After collection, samples were centrifuged and excess water was removed, frozen in a -20 freezer and freeze-dried to be transported to the Netherlands for further analysis. To remove marine salts, the freeze-dried samples were resuspended in Milli-Q water, centrifuged again, and the supernatant was carefully pippeted out, after which samples were freeze-dried again. Freeze-dried samples were weighed with a high-precision microbalance ±0.1 mg resolution), and an uncertainty of ±0.0001 g was applied to all mass measurements. Carbon and nitrogen percentages were measured with a precision of ± 0.02%. These uncertainties were propagated through all derived fluxes, resulting in mass flux values reported to two decimal places, and Corg and total N flux values reported to two and three decimal places, respectively. Grain-size measurements and silt/clay percentages were obtained using laser diffraction, with instrument precision better than 1 μm and 0.1%, respectively. The final calculated grain-size measurements and silt/clay percentages are reported to two decimal places.

2.4 Organic carbon and nitrogen content

Organic carbon and total nitrogen contents were measured using an Elementar Vario El Cube elemental analyzer (EA; Elementar Analysensysteme GmbH, Germany) coupled to an Isoprime vision isotopic ratio mass spectrometer (IRMS; Elementar Analysensysteme, GmbH, Germany) at the University of Amsterdam. Prior to analysis, dried suspended particulate matter from the traps was ground using an a agate mortar and pestle to homogenize. Subsequently,





samples were transferred into silver cups and weighed. The day before measuring, inorganic carbonates were removed by repeated treatment with 1 mol L⁻¹ hydrochloric acid until effervescence stopped. The silver cups were dried overnight on a heating plate and closed the following day with tweezers. For carbon and nitrogen content analyses, three out of the six replicates collected per location and time point were randomly selected for measurements.

2.5 Grain-size analysis

Grain-size analyses were conducted using a Beckman Coulter laser diffraction particle sizer LS13 320. Prior to analysis, 2 mL of sodium pyrophosphate (Na₄ P₂ O₇ · 10 H₂O) was added to each sample, followed by brief sonication for 10 min to ensure complete disaggregation of any remaining particle aggregates. Degassed water was used during the analysis to reduce the impact of gas bubbles, and a magnetic stirrer was used to keep the sample homogenized. The particle-size distributions were categorized into 92 size classes, ranging from 0.375 to 2,000 μ m. Testing with internal glass-bead standards demonstrated a reproducibility of better than 0.7 μ m for mean particle size and 0.6 μ m for median particle size (1 σ). The average standard deviation across all size classes was within 4 vol.%. following Van Der Does et al. (2016).

2.6 XRF elemental analysis

X-ray Fluorescence (XRF) was employed as a non-destructive method to assess elemental composition in SPM samples, performed with an Avaatech scanner at NIOZ. Sub-samples (triplicate) were taken from the Milli-Q-washed, freeze-dried sediment trap samples (see Section 2.3) and homogenized and ground with a pestle and mortar to a fine particle size. The samples were placed in sample holders with a 6 mm radius, following the procedure of Korte et al. (2017). The XRF analysis was carried out using two energy settings: 10 kV for aluminum (AI), silicon (Si), sulfur (S), iron (Fe), and manganese (Mn), and 30 kV for nickel (Ni), bromine (Br), and lead (Pb). For the 10 kV measurements, a current of 1500 µA was applied for 20 seconds without a filter, while the 30 kV measurements used a 500 µA current for 20 seconds with a palladium filter to optimize detection. To check precision of our analyses, one external reference standards (SARM 2) was measured repeatedly and we calculated the coefficient of variation (CV%) per element for one of the standards (SARM 2), which was consistently below 4%. Each sample was analyzed three times to assess internal variability. Data was processed using bAxil spectrum analysis software (developed by Brightspec).





214

215

216

217

218219

220

221

222

223

224

225

226227

228

229

230

231

232

233

234235

236

237238

240241

2.7 Statistical analysis

First, outliers of mass, carbon, and nitrogen fluxes were identified and removed following robust statistical methods for outlier detection, using the median absolute deviation (MAD) approach as described by Rousseeuw and Hubert (2011). This resulted in the removal of 15 mass flux values out of 274 datapoints (5.5 %). These outliers corresponded to exceptionally low fluxes, which were caused by physical obstruction, specifically, shells clogging the sediment trap funnels and preventing material from entering the collection tubes, as observed during sample retrieval. We used the two-sample t-test (independent samples t-test) to compare the means of mass, carbon and nitrogen fluxes, grain size and silt and clay % between wet and dry seasons for each location separately. Prior to analysis, data were checked for normality using the Shapiro-Wilk test and visually assessed using Q-Q plots. Most variables were not normally distributed. For non-normally distributed variables, we applied the nonparametric Kruskal-Wallis test followed by pairwise Wilcoxon rank-sum tests with Bonferroni correction. For normally distributed variables, we used one-way ANOVAs followed by Tukey's Honest Significant Difference (HSD) post-hoc tests to assess differences between locations in the dry and wet seasons. These analyses were conducted separately for each season and applied to grain size, as well as mass, Corg, and total N fluxes. Statistical significance was determined using a threshold of p < 0.05.

Elemental counts obtained from XRF analysis were normalized to account for variability in physical material properties (e.g., density) and measurement conditions (e.g., detector live time). Normalization was performed by calculating centered log-ratios (CLR) of elemental intensities, following the method described by Bertrand et al. (2024). This approach addresses non-linear matrix effects and ensures comparability between measurements. The CLR transformation involves dividing the intensity of each element by the geometric mean of intensities of all selected elements from the same measurement. The geometric mean is calculated as:

239
$$g(z) = \sqrt{Counts_{Element\ A\ (z)} * Counts_{Element\ B\ (z)} * ...Counts_{Element\ n\ (z)}}$$

where *n* is the total number of selected elements. The CLR value for a specific element is then computed as:





242
$$CLR A (z) = \ln\left[\frac{Counts Element A(z)}{g(z)}\right]$$

Only well-measured elements free of noise and zero values were included in the centered logratio (CLR) transformation. Principal Component Analysis (PCA) was then performed on the CLR-transformed elemental data to identify the dominant geochemical processes contributing to differences in sediment composition. Element loadings were used to identify groups of elements with high contributions to the total variance along the first two principal components (PC1 and PC2) using a scree plot. To account for the potential impact of differences in dilution due to a variable terrigenous input, trace metals (e.g., Pb, Ni, Y, Rb, and Cu) were not CLR-transformed, but instead expressed as the Ln of ratios to Al (e.g., Ln (Pb/Al), Ln (Ni/Al)) (Weltje and Tjallingii, 2008). For visualization, average cluster values were calculated per location and season.

To explore the relationship between SPM characteristics and environmental processes across locations and seasons, a Redundancy Analysis (RDA) was performed. In this analysis, response variables (i.e. Mass, Corg and total N fluxes, grain size, silt and clay % and CLR of elemental

lo explore the relationship between SPM characteristics and environmental processes across locations and seasons, a Redundancy Analysis (RDA) was performed. In this analysis, response variables (i.e. Mass, C_{org} and total N fluxes, grain size, silt and clay % and CLR of elemental intensities) were modeled as a function of explanatory variables (e.g., rainfall, wind speed, wind direction, distance from land and from the bay mouth). For this analysis, the locations East 8m and 18 m were combined as East, and West 8 m and 18 m were combined as West, as there were no clear differences between the different depths when examining the RDA results. Before performing the RDA, correlations among explanatory variables were assessed, and highly correlated variables were removed to reduce multicollinearity. All variables were auto-scaled and mean-centered, and as suggested by Shrestha and Kazama (2007), only RDAs with eigenvalues greater than 1 were considered significant. Additionally, a k-means clustering algorithm was applied to the site scores, revealing distinct groups within the dataset.

In addition, we determined the relationships between various environmental and SPM variables, by conducting a Spearman correlation analysis for three locations (East, West, and Mouth) within the study area using data of the wet and dry season. Spearman correlations were chosen as most of the variables were not normally distributed. The variables included CLR of elemental intensities, SPM properties (i.e. grain size, silt and clay ratio, mass, C_{org} and total N fluxes), and environmental factors (i.e. rainfall, wind speed and direction and depth). We categorized correlation (Spearman's rho, r_s) strengths as strong ($r_s > 0.6$) and very strong



274

275

276

277

278279

280281

282

283

284285

286287

288

289

290

291292

293

294

295

296

297298

299

300



 $(r_s > 0.8)$, while weak to moderate correlations were excluded from the visualizations. All statistical analyses and graphing were performed in R (R-CoreTeam 2012) using RStudio (RStudioTeam 2015).

3. Results

3.1 Environmental parameters: seasonal and spatial differences

Environmental data revealed distinct differences between the dry and wet seasons (Fig. 2). During the dry season (April-May 2023), recorded water temperatures at 10 m water depth of the eastern and western reef varied from 26.5-28.8°C, with the highest temperatures observed between April 24 and May 2, coinciding with the transition from spring tide to neap tide. Rainfall during this period was minimal, with only two notable events: 4 mm on May 14 and 2 mm on May 22. In contrast, the wet season (October-November 2023) showed higher water temperatures, exceeding 30°C from October 28 to November 11 and averaging approximately 29°C throughout the rest of November. Rainfall was substantially higher than in the dry season, with precipitation recorded on nearly every sampling day. The most intense rainfall occurred between October 25 and November 6, peaking at 24 mm on November 2. Wind also showed distinct seasonal patterns. The dry season was characterized by consistent southeasterly winds with high average speeds of approximately 20 m s⁻¹, reaching peaks of 27.4 m s⁻¹. The wet season exhibited more variable wind directions, predominantly from the southeast as well, with occasional extreme shifts (e.g., the change in direction recorded on November 20). Wet season wind speeds were notably lower, averaging around 15 m s⁻¹, particularly in early October, though they increased by mid-November. The wet season also showed a relationship between precipitation events and wind patterns, with lower wind speeds often coinciding with heavier rainfall. In addition to seasonal environmental differences, the ADCP data revealed spatial variations in water flow between the eastern and western reefs (Fig. 2). Current velocities were notably higher at the western reef, ranging from 0.01 to 0.07 m s⁻¹, compared to the eastern reef, where velocities ranged mostly from 0.005 to 0.02 m s⁻¹. Although limited dry season data prevented robust seasonal comparisons, water velocities remained within similar ranges across both seasons





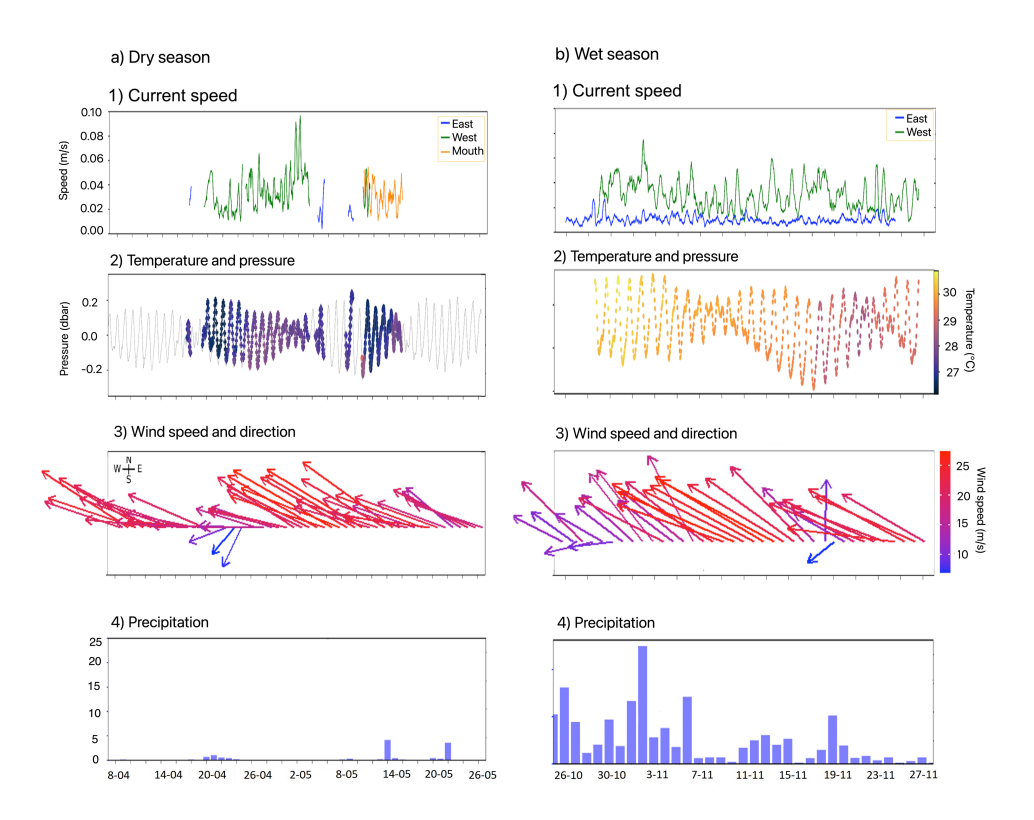


Figure 2. Environmental variables during the sampling periods in the dry and wet seasons. Panels a) shows current speed over time at the western reef at 8 m (green), eastern reef at 8 m (blue) and mouth at 3 m (only in the dry season; orange). Panels b) show water pressure at 10 m in the reef in dbar (reflecting tidal cycles) and water temperature in °C, the latter represented by a color scale. Panels c) show wind speed (color of the vectors) and direction. Panels d) show rainfall (mm).

3.2 Seasonal and spatial averages of fluxes and grain size

Properties of SPM showed clear spatial and seasonal patterns (Table 1). In the dry season, fluxes (total mass, organic carbon (C_{org}), and total N) were significantly higher at the mouth than at the reef locations (Tables 1, S1). In the western reef, SPM had a larger grain size (with a significantly lower proportion of silt and clay) compared to the east and the mouth (Tables 1, S1). In the wet season, the mouth exhibited the highest fluxes, with higher silt and clay contents compared to the material found at the other locations (Table S1). At most sites, mass, C_{org} and total N fluxes were higher in the wet season compared to the dry season, except for west 18 (Table S2). The mouth showed the strongest seasonal signal: fluxes were 3–4 times





higher in the wet season and grain size was significantly smaller than in the dry season (Table 1, S2).

At the east reef, seasonal differences were also evident, especially at 8 m, where mass fluxes doubled, and C_{org} and total N fluxes increased fourfold in the wet season. At 18 m, this seasonal increase in fluxes was more modest, but still clear (Table S2).

Western reefs showed a mixed pattern. At 8 m, fluxes increased in the wet season, while at 18 m, they were higher in the dry season, contrasting with the other locations. Nonetheless, average grain size was smaller, and silt and clay contents were higher in the wet season across all reef sites (i.e. eastern and western reef; Table 1, S1, S2). In particular, during the dry season, the western reef had the lowest portion of silt and clay (28–38%), which was significantly lower than at the eastern reef (51–53%).

Table 1. Summary of the mean (highest between seasons per site in bold), maximum and minimum values of mass, C_{org} and total N fluxes (g m⁻² d⁻¹), grain size (μ m), silt and clay % measured at the mouth east 8 and 18 m, and west 8 and 18 m during the dry and wet season. Asterisks show significant differences between seasons (See Tables S1 and S2 for full statistical analyses between locations and seasons, respectively).

		Mouth		East 8 m		East 18 m		West 8 m		West 18 m	
		Dry	Wet	Dry	Wet	Dry	Wet	Dry	Wet	Dry	Wet
Mass flux (g m ⁻² d ⁻	Mean	8.47	36.32*	5.35	9.52*	6.60	8.99	5.23	10.61	7.48	5.23
1)	Max	24.11	84.43	6.54	18.74	11.75	36.61	13.28	39.45	12.93	15.12
	Min	1.56	16.65	2.27	1.16	3.53	0.97	1.31	2.58	3.31	2.07
C _{org} flux (g m ⁻² d	Mean	0.18	0.61*	0.05	0.17	0.09	0.21	0.06	0.11	0.12	0.09
1)	Max	0.53	0.17	0.09	0.49	0.18	0.55	0.20	0.63	0.24	0.16
	Min	0.03	0.26	0.01	0.03	0.05	0.06	0.04	0.04	0.04	0.04
Total N flux (g m ⁻² d ⁻	Mean	0.031	0.082*	0.007	0.031*	0.012	0.021	0.022	0.033	0.022	0.012
¹)	Max	0.081	0.233	0.011	0.074	0.024	0.083	0.085	0.112	0.043	0.023
	Min	0.004	0.031	0.001	0.007	0.007	0.012	0.005	0.005	0.008	0.004
Grain	Mean	45.53	31.46	62.62	51.17	85.96	35.41	86.46*	42.88	95.34*	43.75
Size	Max	74.85	52.05	279.46	81.10	273.09	54.79	125.05	60.74	159.49	62.28
(µm)	Min	36.09	23.52	27.35	27.81	26.16	11.65	36.09	25.08	25.62	15.96
Silt and	Mean	61.67	75.06	52.96	55.30	51.69	61.84	38.16	62.41*	28.65	57.00*
Clay %	Max	79.93	96.54	72.03	77.18	77.40	88.79	58.06	79.41	40.54	81.92
	Min	49.45	50.40	25.14	35.59	37.27	47.63	25.52	43.40	22.21	39.82





3.3 Seasonal trends of mass fluxes and SPM properties

3.3.1 Mouth

Fluxes at the mouth exhibited temporal variability within each season. During the dry season mass, C_{org} , and total N fluxes remained relatively stable over time. In contrast, during the wet season, fluxes were significantly higher and associated with a finer grain-size distribution (Fig. 3, Table 1). The proportion of fine particles (0–20 μ m) and silt (20–63 μ m) increased in the wet season, while the proportion of fine-to-medium sand (63–150 μ m) and coarser sand (>150 μ m) decreased compared to the dry season (Fig. 3). The highest fluxes observed at the mouth (~70 g m⁻² d⁻¹) directly followed a heavy rainfall event on November 2nd. At this time, the average grain size of settled material was particularly small (~24 μ m), with the fine particles and silt making up ~80% of the material.



346

347

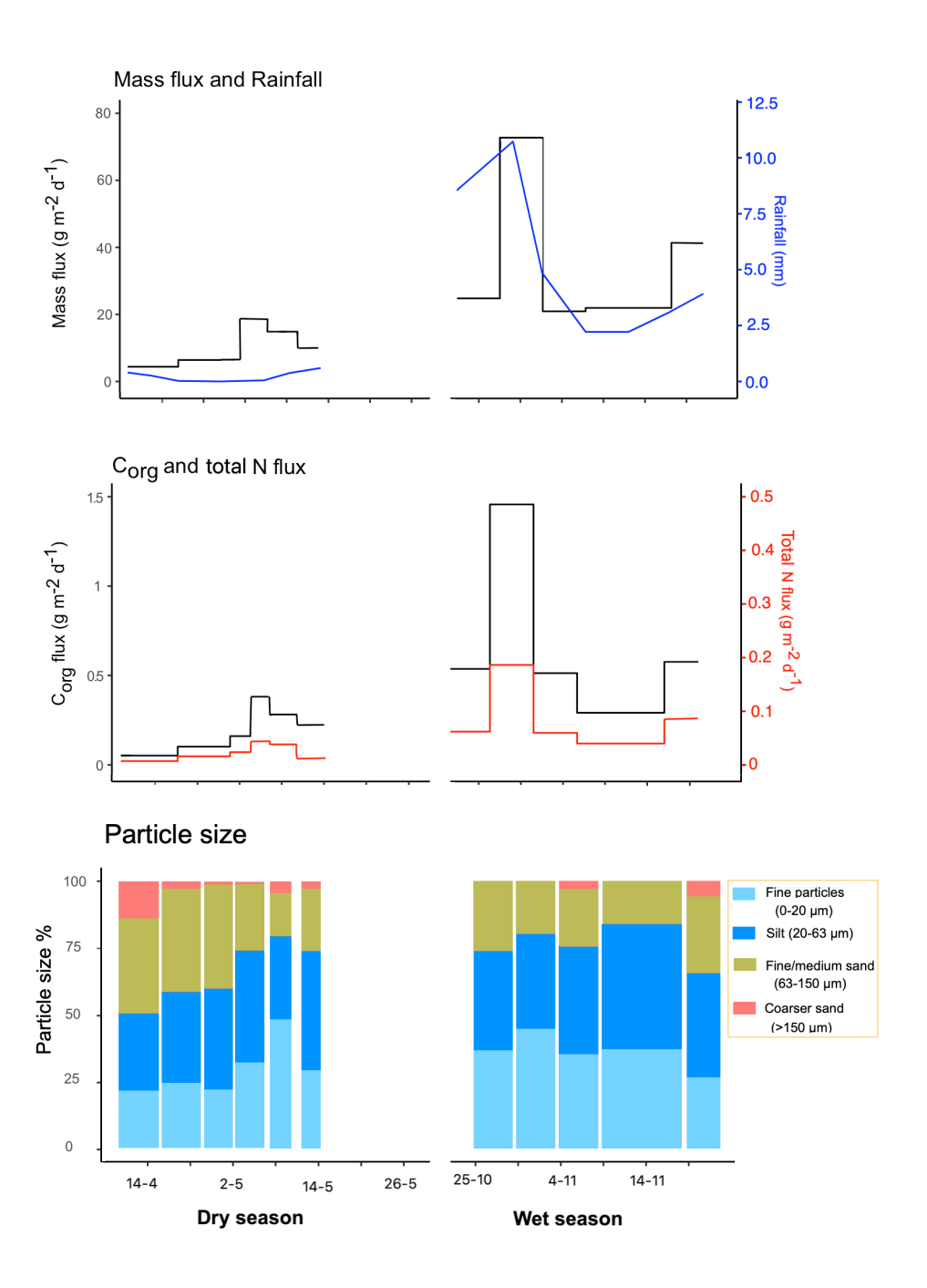


Figure 3. SPM fluxes and grain-size characteristics of the mouth of the dry season and wet season. The first panel shows mass (g m^{-2} d^{-1}) and average rainfall (mm). Second panel shows C_{org} and total total N fluxes (m^{-2} d^{-1}). Note that mass, organic carbon, and total nitrogen flux





scales are different than in Figure 4 and 5. Bottom panel shows the % of fine particles (0-20 μ m) silt (20-63 μ m), fine-medium sand (20-150 μ m) and coarser sand (>150 μ m).

3.3.2 East 18 and 8 m depth

At the eastern reef, and a depth of 8 m fluxes remained relatively constant throughout most of the sampling period in the dry season (Figure 4.a). Here, mass flux increased during May 2–16, although Corg and total total N fluxes did not show a corresponding increase. At 18 m water depth there was higher variation during the sampling perios. Also at this depth, the highest mass, Corg and total total N fluxes were recorded towards the end of the sampling period (May 16–24). Grain-size composition was constant during the whole sampling period at both 8 and 18 m.

Over the wet season sampling period, the lowest mass, Corg and total N fluxes were recorded from October 25–31 (mass flux: 2–5 g m⁻² d⁻¹, Corg flux: 0.06–0.1 g m⁻² d⁻¹ and total N flux: 0.004–0.01 g m⁻² d⁻¹), while relatively high fluxes occurred from October 31–November 5 (mass flux: 12-15 g m⁻² d⁻¹, Corg flux: 0.3-0.4 g m⁻² d⁻¹ and total N flux: 0.04-0.05 g m⁻² d⁻¹), coinciding with the highest rainfall event of the sampling period (November 2). During this high-rainfall period, SPM exhibited smaller grain size, and a higher percentage of silt and clay similar to what was observed at the mouth. At both depths, the proportion of coarser sand

(>150 µm) was lower in the wet season compared to the dry season.



369 370

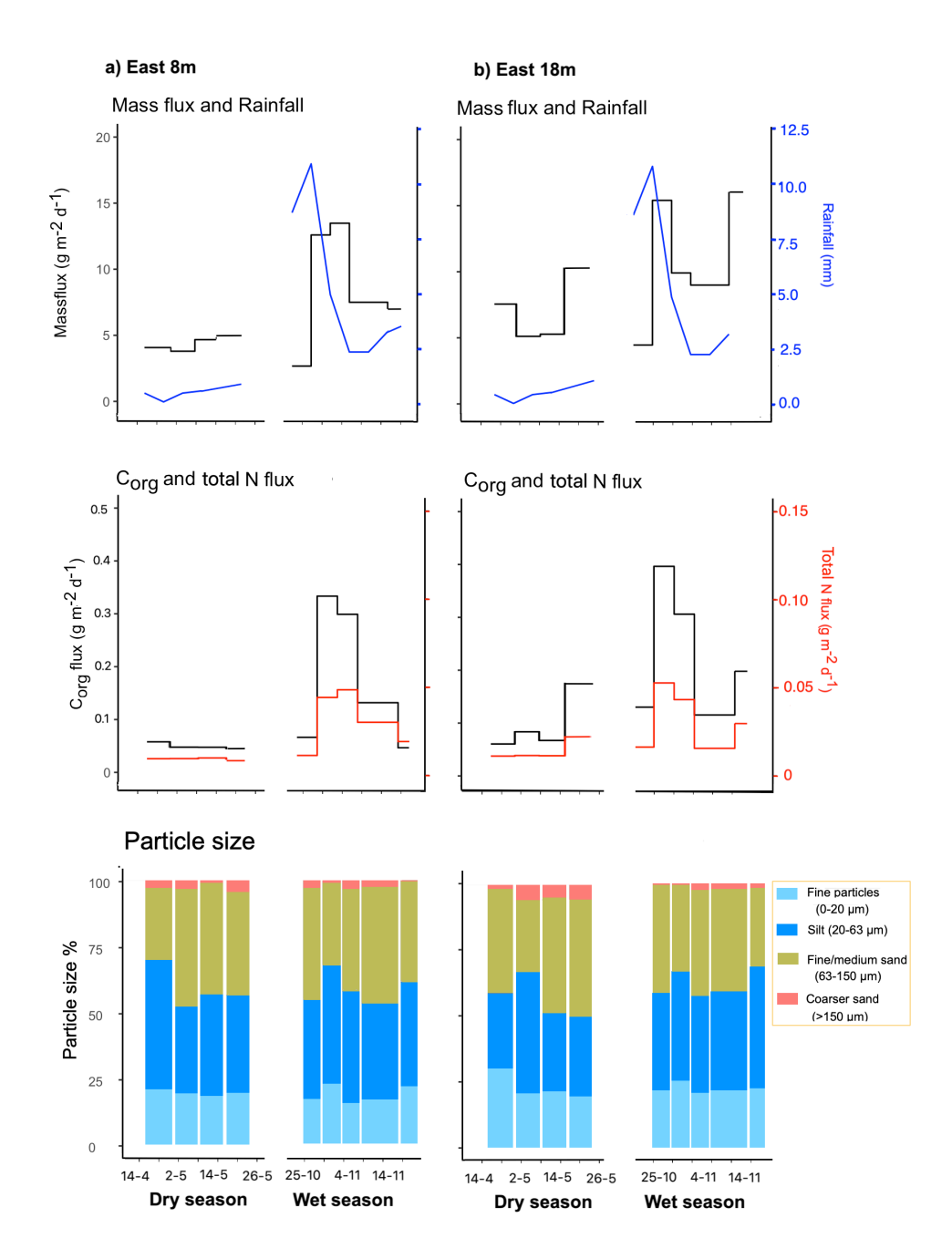


Figure 4. SPM fluxes and grain size of the a) East 8m and b) East 18m of the dry season and wet season. The upper panels show mass fluxes (g m $^{-2}$ d $^{-1}$) and average rainfall (mm). Middle panels show C_{org} and total total N fluxes (g m $^{-2}$ d $^{-1}$). Bottom panel shows the proportion of fine





particles (0-20 μ m) silt (20-63 μ m), fine-medium sand (20-150 μ m) and coarser sand (>150 μ m).

3.3.3 West 18 m and 8 m depth

Seasonal differences at the western reef were less pronounced compared to those observed at the other locations. At 18 m, mass, C_{org} , and total total N fluxes remained relatively stable both within and between seasons (Fig. 5). However, the material was coarser at this site in both seasons, with a higher proportion of coarse sand (>150 μ m) than at the mouth and eastern reef. This coarser fraction was particularly dominant in the dry season. At 8 m, mass, C_{org} , and total total N fluxes showed a clear seasonal difference. During the dry season, highest mass flux was recorded between May 8 and 18 (~13 g m⁻² d⁻¹), coinciding with one of the few rainfall events in that period (May 14). In the wet season, fluxes at 8 m displayed greater temporal variation, with peak values around the intense rainfall on November 2 (mass flux: 18 g m⁻² d⁻¹; C_{org} flux: 0.3 g m⁻² d⁻¹; total N flux: 0.05 g m⁻² d⁻¹). Grain-size analysis showed that the percentage of fine particles (0–20 μ m) and silt (20–63 μ m) was higher in the wet than in the dry season, particularly at 8 m. In contrast, the proportion of coarser sand was lower in the wet season and generally higher at both 8 and 18 m compared to the mouth and eastern reef. At 18 m, mass fluxes were lower than at all other locations (i.e., West 8 m, East 8 m and 18 m, and the mouth).



391

392

393

394 395



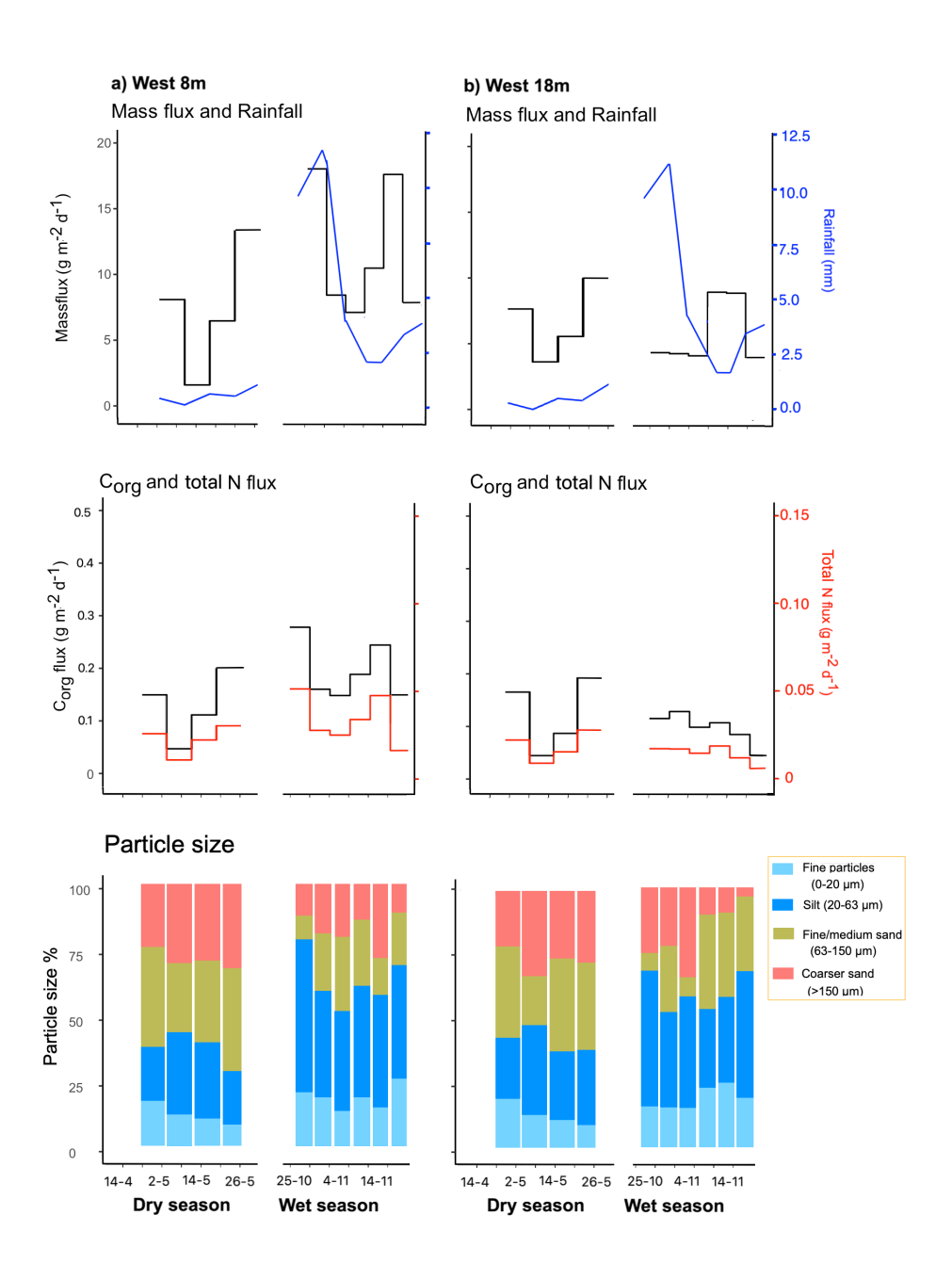


Figure 5. SPM fluxes and grain size of the a) West 8m and b) West 18m of the dry season and wet season. Upper panels show mass fluxes (g m⁻² d⁻¹) and average rainfall (mm). Middle panels show C_{org} and total total N fluxes (g m⁻² d⁻¹). Bottom panel shows the % of fine particles (0-20 μ m) silt (20-63 μ m), fine-medium sand (20-150 μ m) and coarse sand (>150 μ m).

3.4 Elemental composition of the suspended matter

https://doi.org/10.5194/egusphere-2025-4873 Preprint. Discussion started: 28 November 2025 © Author(s) 2025. CC BY 4.0 License.





A principal component analysis (PCA) was performed to identify the largest patterns in the settled material elemental composition (Fig. 6). This revealed four distinct clusters of elements: the first cluster, comprising Si, Mn, Ti, Al, Co and Fe (purple circle Fig. 6), reflects a dominant terrigenous origin probably related to runoff, with their distribution being most pronounced at the bay mouth and east reef locations. A second cluster, consisting of Ni, Y, Rb, Pb, and Cu (green circle Fig. 6), consists of trace elements generally associated with pollution, which were found in elevated concentrations particularly at the reef sites. A third cluster, defined by Br, S, Cl, and Mg (red circle Fig. 6), consists of elements typical of marine organic matter and/or salts indicating a strong seawater influence, likely reflecting regions with higher marine impact, such as at the western reef. A fourth, less well-defined cluster included Sr, Ca, Zn, and Zr (blue circle Fig. 6), elements associated with marine carbonates (Ca and Sr) as well as terrigenous (Zr) and pollution (Zn) sources. As this cluster is located central in the PCA space it is likely not specifically related to any of these factors.



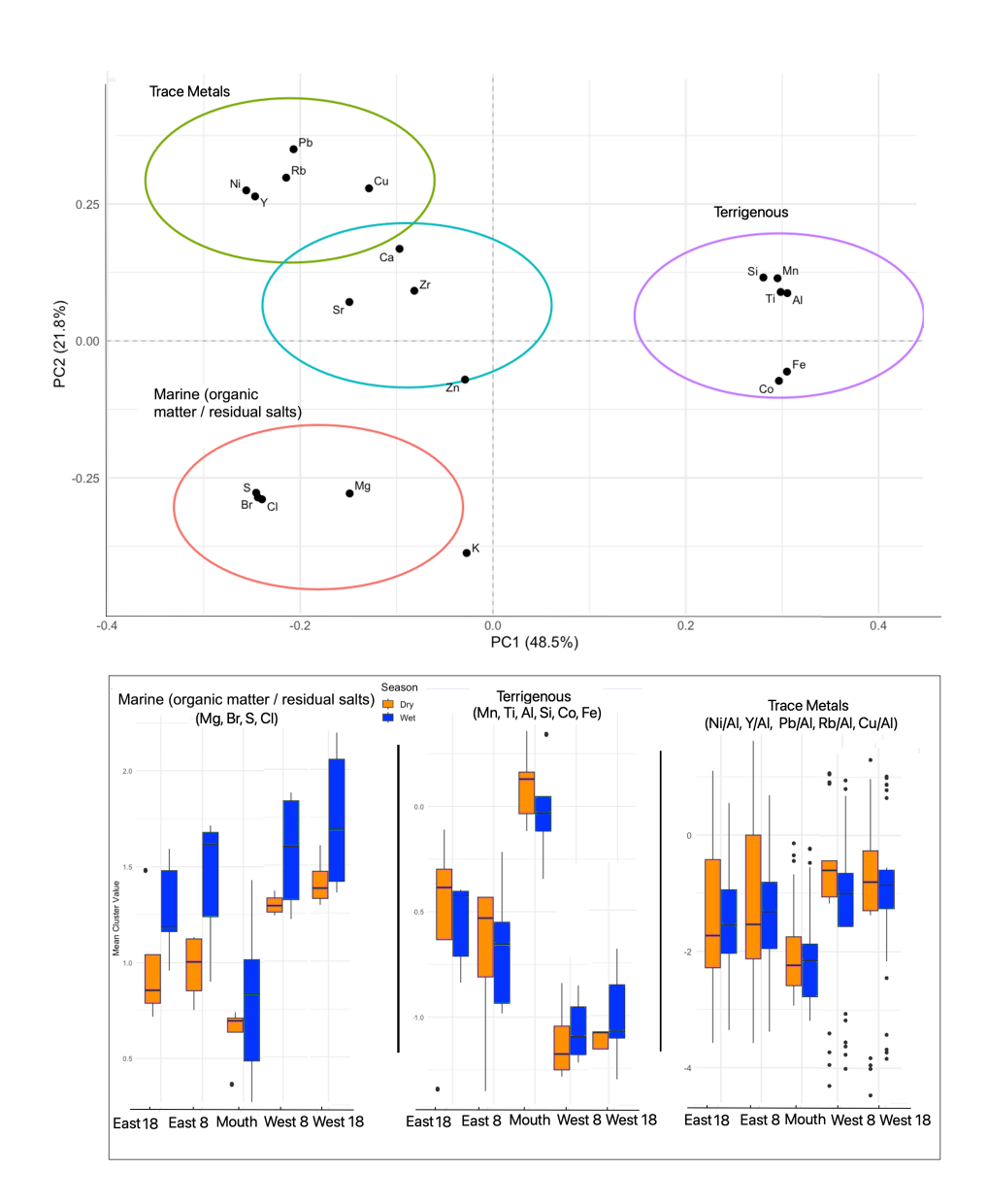


Figure 6. Principal Component Analysis (PCA) cross plot of PC1 (48.5%) and PC2 (21.8%) showing the loadings of XRF-derived elemental ratios. Four distinct element clusters are visible: (1) a terrigenous cluster (Si, Mn, Ti, Al, Co, Fe) loading positively on PC1; (2) a trace metal cluster (Ni, Y, Rb, Pb, Cu) with positive loadings on PC2 and negative on PC1; (3) a marine cluster typically associated to organic matter and/or residual salts (Br, S, Cl, Mg); and (4) a fourth group (Sr, Ca, Zn, Zr) with unclear affiliation. Spatially, the terrigenous elements were more prominent at the bay mouth and east reef, trace metals were highest at the east reef, and marine salt elements dominated the western reef.





3.4.1 Seasonal and spatial trends of elemental compostion and correlations of SPM 421 422 characteristics with environmental parameters 423 XRF analysis revealed distinct relative spatial differences in the composition of SPM (Fig. 7). 424 Aluminum (AI), an element associated toterrigenous input, displayed the highest intensities 425 at the mouth, and eastern reef, and the lowest at the western reef. This spatial pattern was 426 consistent across both seasons. During the wet season Al values increased following periods 427 of intense rainfall (25 October-8 November, Fig. 2). Other terrigenous elements showed 428 similar trends (Fig. S1). In contrast, the Pb/Al ratio, indicative of anthropogenic pollution, was 429 highest in the western reef, lowest at the mouth and showed intermediate values in the east. This pattern held for both seasons and was consistent across other trace metal ratios (Fig. S2). 430 The Ca/Fe ratio, reflecting the relative contribution of marine carbonate versus terrigenous 431 432 inputs, exhibited a similar spatial pattern, with the highest values found in the western reef, intermediate values in the east, and the lowest at the mouth. Additionally, Ca/Fe values were 433 434 higher during the dry season, showing a greater influence of marine carbonate inputs during periods of reduced runoff. 435 436 Correlations between SPM properties and environmental drivers confirmed these spatial contrasts (Fig. S3). At the mouth, mass, Corg, and total N fluxes were strongly intercorrelated 437 (>0.9) and closely linked to Al, Si, Mn, and Fe, indicating a dominance of fine-grained, 438 439 terrigenous material. Rainfall and wind also correlated with fluxes during the wet season. At the eastern reef, fluxes were again intercorrelated, but showed weaker associations with 440 441 rainfall. Correlations with Fe and Mn point to a stronger influence of silt and clay fractions. In contrast, at the western reef, fluxes correlated less with environmental drivers, but grain size 442 showed a stronger role. Here, coarser particles were occasionally linked to higher mass and 443 444 organic matter fluxes in the dry season, whereas in the wet season fluxes were more 445 influenced by fine-grained material and terrigenous elements such as Al and Fe.





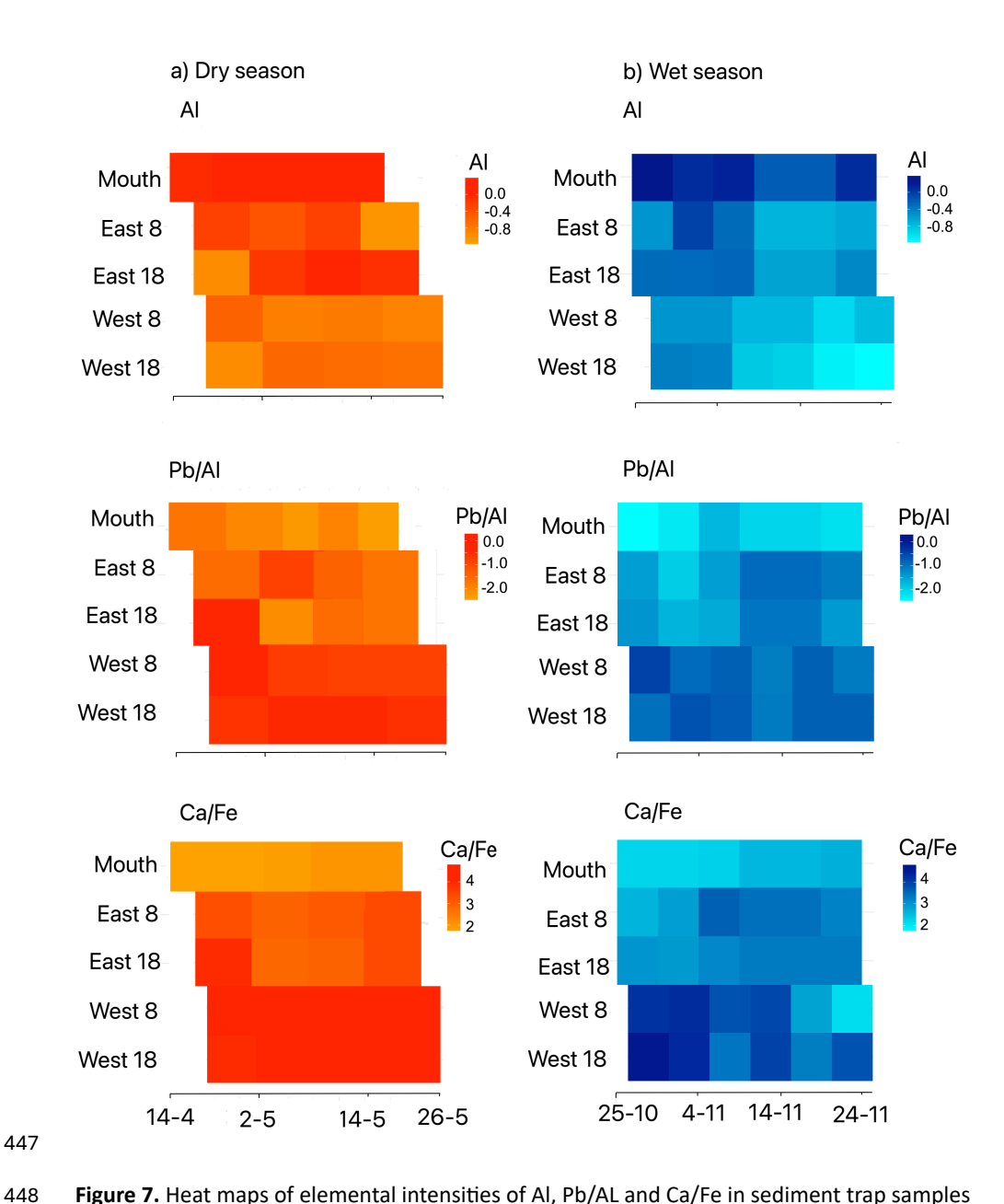


Figure 7. Heat maps of elemental intensities of Al, Pb/AL and Ca/Fe in sediment trap samples during the a) dry season and b) wet season. The x-axis represents sampling dates, and the y-axis displays the five sampled locations (Mouth, East 8, East 18, West 8 and West 18 m). The color scale indicates the centered log-ratios (CLR) of elemental intensities for Al and log-ratios for Pb/Al and Ca/Fe.

4. Discussion

449

450

451

452 453



456 457

458

459

460

461 462

463

464

465 466

467

468

469 470

471

472473

474

475

476 477

478

479 480

481

482

483 484

485



Near the bay's mouth, the highest fluxes of suspended matter (SPM) were found and this material was finer with elevated values of terrestrial elements (Si, Fe, Al, and Mn) than in locations further away from the bay. In contrast, the location west of the bay's mouth showed lower concentrations of SPM and the settled material was coarser grained with higher values of Pb, Ni, and Cu. These spatial differences show that the suspended matter near the bay's mouth and eastern reef is primarily influenced by material derived from terrestrial runoff, whereas the western reef reflects a stronger open-ocean and more marine signature. Notably, despite receiving less terrestrial input, the reef sites—particularly the western reef—showed the strongest signals of anthropogenic pollution (e.g., Pb, Rb, Cu, Ni), suggesting that fluxes and deposition are decoupled and that contaminants accumulate preferentially at these sites. Differences between seasons are caused by changes in runoff due to variations in rainfall and wind regimes.

4.1 Bay influence and marine processes

The influence of Piscadera Bay on SPM content in nearshore waters reveals a clear spatial and temporal pattern. At the bay mouth, highest mass fluxes, elevated organic content, and finest particles were found. While comprehensive studies using sediment traps to examine spatial gradients in suspended particulate matter characteristics in bay-reef systems remain scarce, this pattern is consistent with findings from other Caribbean coastal systems, where sediment accumulation rates show strong spatial gradients related to proximity to terrestrial sources (Toro et al., 2021). Similarly, the Magdalena River system in Colombia, which discharges exceptionally high sediment loads directly into the Caribbean Sea, illustrates how major terrestrial inputs create pronounced sediment flux gradients in Caribbean coastal waters, with higher amounts and finer material found close to the river mouth (Restrepo et al., 2014). The elemental composition, particularly the high values of Si, Al, Mn, Co and Fe in this study, point to a terrestrial origin of SPM as these lithogenic elements are fundamental markers of soil erosion and terrestrial runoff (Larson et al., 2015). Together these findings show a transition from mainly terrestrial input to more marine influenced SPM dynamics (indicated by fluxes and XRF elements) with increased distance from the bay. This pattern aligns with several studies showing that SPM concentrations and their negative effects on coral reefs decrease with distance from sources, such as rivers or bays (Fabricius, 2005; Rogers and Ramos-Scharrón, 2022; Storlazzi et al., 2011).

https://doi.org/10.5194/egusphere-2025-4873 Preprint. Discussion started: 28 November 2025 © Author(s) 2025. CC BY 4.0 License.



486 487

488

489

490

491 492

493

494

495

496 497

498 499

500501

502

503

504

505

506

507

508 509

510511

512

513

514

515

516



East of the bay mouth, the suspended matter shows more impact of the bay system compared to the western reef, however less pronounced than at the mouth. This alignes with Sánchez Baranco et al. (2025), showing that bay-derived characteristics, such as dissolved-nutrient concentrations, salinity, and temperature attenuate with increasing distance from bays. The eastern reef, particularly at 8 m depth, presents a recognizable bay signature through elevated carbon and nitrogen content and relatively high values of elements, such as Al, Si or Fe, indicating terrestrial runoff. The low current speeds measured at the eastern reef (8 m depth; Fig. 2) can explain this accumulation of finer material with higher organic content, creating a zone where bay influence lasts longer due to longer residence times. Safak et al. (2015) demonstrated through modeling that in areas surrounding shallow coastal bays—particularly near inlets where water circulation is restricted—tidal forces can enhance material accumulation. This pattern is supported by our data, showing elevated concentrations of terrigenous elements (Fig. 7) at the mouth and eastern reef, and strong correlations between water pressure (used here as a proxy for tidal variation, Fig. S3) and both mass fluxes and coarser material, especially at the bay mouth. This likely indicates that during periods of higher water pressure, such as high tide or spring tide, larger quantities of suspended matter, including coarser particles, are transported near the mouth of the bay. The western reef, positioned furthest from Piscadera Bay, reveals different patterns compared to the mouth and eastern reef. This site is characterized by less variability in fluxes of mass, Corg, and total N. The consistently higher Ca/Fe found here further suggest a stronger marine signal at this site compared to the mouth and eastern reef, reflecting greater contributions of

to the mouth and eastern reef. This site is characterized by less variability in fluxes of mass, C_{org} , and total N. The consistently higher Ca/Fe found here further suggest a stronger marine signal at this site compared to the mouth and eastern reef, reflecting greater contributions of carbonate-rich marine particles relative to terrigenous inputs (Nizou et al., 2011). However, this location shows relatively high values of Br, S, Pb, and Ni. Trace metals were found at both reefs, but values were consistently higher at the western reef, particularly for Pb and other pollution indicators (Figs. 7, S2). These trace elements suggest a complex interplay of marine biological activity and potential anthropogenic influences, with origins ranging from marine organism decomposition to maritime and industrial processes (Caballero-Gallardo et al., 2020; Fernandez et al., 2007). The presence of Pb and Ni indicates potential anthropogenic input, such as maritime activities, or coastal infrastructure (Nalley et al., 2021; Fernandez et al., 2007) and corroborates with high anthropogenic input found related to the close proximity of Piscadera Bay to urbanized areas around Willemstad, the largest city on Curação (Van de



518519

520521

522

523

524

525

526

527

528

529

530531

532

533

534

535536

537

538

539 540

541 542

543 544

changes in environmental conditions.



Loosdrecht, submitted). The presence of pesticides, or industrial processes and persistence and accumulation of these elements at the western reef may be partly explained by the site's three-dimensional reef structure, which can act as an efficient trap for suspended and settling particles. Greater structural complexity increases the capacity of the reef to retain material, allowing for longer particle residence times and the potential for local enrichment of both natural and anthropogenic elements (Ng et al., 2022; Bothner et al., 2006). Hydrodynamics also shape the conditions for suspension and settling of particulate matter at this site, with current speeds higher than those in the eastern reef (Fig. 2). The effect of current speed appears to be depth-dependent: at 8 m water depth we still observe bay or land influence, as evidenced by fluctuating fluxes during the wet season that correspond with rainfall events (Fig. 5). However, at 18 m water depth, this effect is not noticable, suggesting diminished influence from surface runoff at greater depths. The higher current velocities affect SPM dynamics by reducing particle settling time and increasing resuspension, resulting in winnowing of fine material from the seabed and increased turbidity in the water column (De Jong et al., 2025; Prochnow et al., 1970; Cuttler et al., 2017). During 2023, the model by (Bertoncelj et al., 2025) identified a high presence of mesoscale eddies in the region, which may have contributed to the transport of particulate material from areas beyond the immediate vicinity of the study site. These spatial and seasonal patterns are further supported by a redundancy analysis (Fig. 8), revealing that approximately 49% of the total variance in SPM characteristics is explained by spatial factors including depth, distance to land, and proximity to the mouth of Piscadera Bay. In line with our results, Jouon et al. (2008) showed that fluxes of suspended particles have higher variability over space than over time. This analysis clearly differentiated the western reef (characterized by marine-associated elements) from the bay mouth (dominated by terrestrial markers), with the eastern reef showing intermediate characteristics. A portion of variance (7%) is attributable to seasonal factors, primarily driven by rainfall, wind speed, and wind direction. This multivariate approach confirms that the bay's influence follows both spatial gradients and responds to seasonal





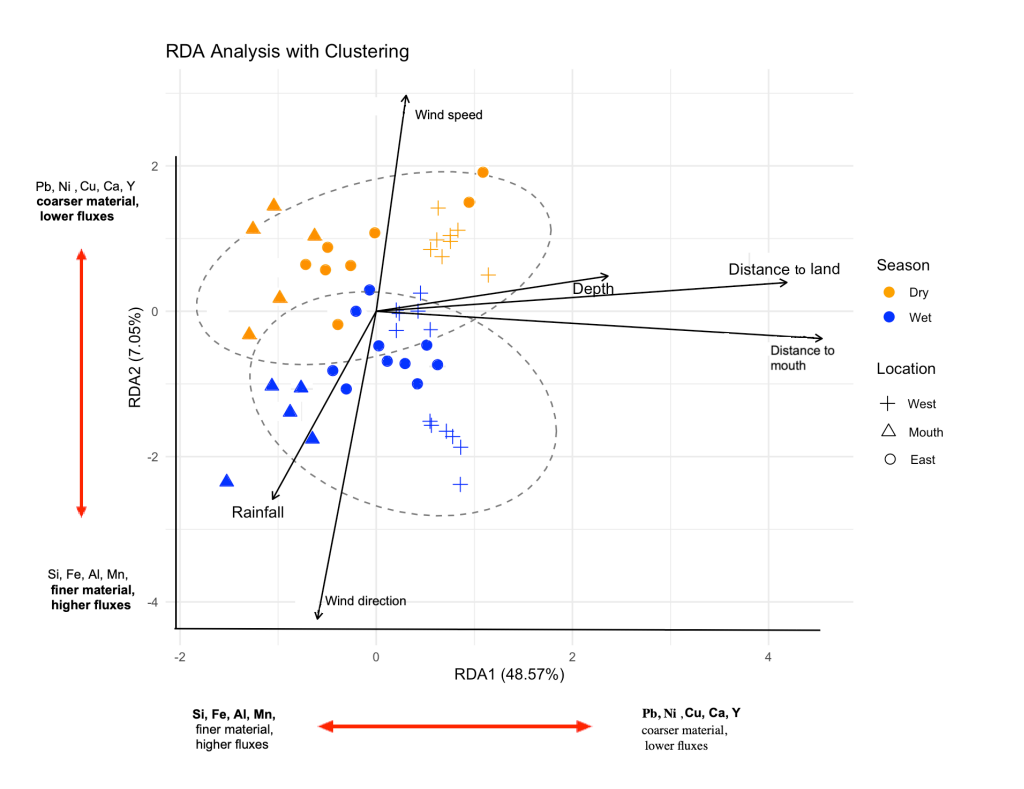


Figure 8. Redundancy analysis (RDA) biplot of sediment trap data collected from three locations in the bay (mouth, East, and West) during dry and wet seasons. Points are colored by season and shaped by location, with ellipses representing clusters at 95% confidence. RDA1 explains 48.57% of the variance and is primarily determined by depth, distance to land, and distance to the mouth, separating the locations. RDA2 accounts for 7.05% of the variance and is driven by rainfall, wind speed, and wind direction, distinguishing between seasons

4.2 Seasonal modulation of processes

Mass fluxes recorded at both reef sites during the dry season fall within the ranges reported for reefs worldwide that are relatively uninfluenced by human activities (i.e., $1-10 \text{ g m}^{-2} \text{ d}^{-1}$) (Rogers, 1990). However, during the wet season, this range is greatly exceeded at both reef sites (except for the western reef at 18 m water depth), with mass fluxes reaching 18–40 g m⁻² d⁻¹. In addition, organic matter fluxes measured in reefs near other bays in Curaçao (e.g. Santa Martha) are half of the fluxes we measured in both the east (8 and 18 m) and west (8 m) during the wet season (De Jong et al., 2025).

The bay mouth exhibits the most pronounced correlations (Fig. S3), particularly during the wet season, where fluxes and elemental concentrations strongly align with rainfall and wind





564565

566

567

568

569 570

571

572

573

574

575

576577

578

579

580 581

582

583

584 585

586

587 588

589

590

591592

593

dynamics. This suggests that the mouth functions as a conduit for terrestrial and marine material exchange, with runoff and hydrodynamics controlling SPM composition. Similar patterns have been observed on other Caribbean islands, with increased presence of elements indicating runoff such as Fe, Si, and Al following rain events (Larson et al., 2015). Although Si can also indicate biogenic silica (i.e. diatoms) (Lobo et al., 2016; Palmer and Abbott, 1986), the alignment of Si with Fe and Al trends suggests it primarily reflects terrestrial runoff in our case. In addition, groundwater in Curação has been shown to contain elevated nitrogen and trace metal concentration in urban areas, largely due to wastewater leakage, and this contaminated groundwater discharges into coastal zones and bays, posing a risk for nutrient enrichtment in these areas (Wit et al., 2025). At the eastern reef, a similar but less pronounced trend is observed, with environmental influences becoming more evident during the wet season. In contrast, the western reef shows minimal correlations in the dry season, indicating that local sedimentary processes such as resuspension likely determine SPM characteristics. Still, correlations increase during the wet season, indicating an increased influence of rainfall-driven processes and enhanced SPM transport in this area as well. East of the bay's mouth, the seasonal variability in suspended matter, both its abundance and composition, is less pronounced than at the mouth. At 8 m water depth, mass fluxes in the wet season were highest. At 18 m however, mass fluxes show no significant seasonal differences although elemental compositions vary consistently between 8 and 18 m water depths, suggesting a depth-dependent gradient in the bay's influence. This vertical variability may be driven by several processes: fine-grained particles originating from the bay or from runoff may settle closer to shore before reaching deeper waters (Mccave, 1975); differences in current speeds or directions between depths may influence the transport and resuspension of particles (Gardner et al., 2018); and other environmental conditions such as stratification or wave-induced mixing may act to retain suspended material at shallow depths. The seasonal and spatial correlation patterns highlight the important role of environmental conditions, particularly precipitation and runoff, in modulating SPM transport and composition (Fig. S3). Recent studies have documented enhanced bay-ocean exchange during the wet season in Curaçao, resulting in increased mobilization and transport of SPM and associated elements along the southwest coast reefs (Sánchez Barranco et al., 2025; Van de





595596

597

598

599

600

601

602

603

604

605

606

607

608

609

610

611

612613

614

615

616

617

618

619 620

621622

623

Loosdrecht et al., submitted). This exchange favors the suspension of finer particles (higher silt and clay), which provide greater surface area for adsorption of metals and organic matter, enriching particle-bound elements such as Cu, Zn, Pb, and Ni (Lakhan et al., 2003; Malarkey et al., 2015; Bergamaschi et al., 1997). Flux-environment correlations were stronger in the wet season, with reef fluxes 2-3 times higher during peak rainfall (Figures 4, 5, 7), consistent with reported seasonal increases (Ismail et al., 2005; Li et al., 2013) and even extreme storm-driven surges (>1000-fold; Risk, 2014). In contrast, reduced exchange in the dry season, as warmer and saltier bay waters accumulate, traps nutrients and pollutants (Sánchez Barranco et al., 2025). Our current-speed data (Figure 2) confirm this seasonal contrast. In the wet season, however, mixing with offshore waters intensifies material export, as reflected in the stronger correlations between fluxes and environmental drivers at the mouth and eastern reef. High rainfall during the 2023 El Niño amplified wet-season dynamics by increasing runoff and wastewater inputs, leading to elevated fluxes (Table 1) and higher Si, Al, Fe, and Mn at the bay mouth (Figure 6). Wastewater management on the island is very limited, with only ~20% of the population connected to sewage systems (Wit et al., 2025). Additional anthropogenic inputs, including the emergency sewage overflow (Govers et al., 2014), deliver organic-rich wastewater to reefs during heavy rainfall, enhancing Corg and total N fluxes and strengthening their correlations with Fe and Mn (Figure 8). Resuspension of polluted bay sediments during

4.3 Ecological implications

The observed SPM flux patterns reveal a clear spatial gradient of terrestrial material input, with potentially significant ecological consequences. Increased eutrophication, sedimentation, and decreased herbivory have been identified as key factors reducing coral resilience (Littler and Littler 1998; Kuffner et al. 2008). Dutra et al. (2006) showed that SPM fluxes higher than 10 g m⁻² d⁻¹, which in our study were recorded in both reefs during the wet season, correlate with lower coral larvae survival and settlement and negatively affect coral growth. The eastern reef, more directly connected to the bay, receives higher concentrations of organic carbon, nitrogen, and lithogenic material compare to the western reef. Fine-grained material can have detrimental effects on reef ecosystems, primarily by altering benthic

the wet season further exposes reef organisms to toxic pollutants (De Jong et al., 2025).





625626

627

628

629

630 631

632

633

634

635

636

637638

639 640

641

642643

644

645 646

647648

649 650

651

652

653 654 conditions and preventing coral larvae stettlement (Risk, 2014; Hodgson, 1990). In addition, increased water turbidity diminishes photosynthetically available radiation, which is crucial for coral and algal photosynthesis (Rogers and Ramos-Scharrón, 2022; Weber et al., 2012; Fabricius, 2005). Although elevated organic content may initially appear beneficial, chronic nutrient enrichment has been shown to exacerbate coral disease prevalence and bleaching (Aronson et al., 2003; Vega Thurber et al., 2014), while also promoting abundances of opportunistic organisms such as turf algae, macroalgae, and bacterial communities that can rapidly colonize available substrate and outcompete corals for space and light resources, ultimately leading to phase shifts from coral-dominated to algae-dominated reef systems (Gorgula and Connell, 2004; Vermeij et al., 2010). In the last decades, studies have shown the effect of these bays in nearby reefs and the properties of the water column. For instance, Govers et al. (2014) demonstrated that other ecosystems, such as seagrass beds, are threatened by eutrophication resulting from emergency wastewater overflow and coastal housing near these bays. Also, recent studies have proven the presence of organic chemical pollution around bays in Curação as indicators of waste water and industrial pollution (De Jong et al., 2025). The SPM dynamics observed in this study provide important insight into the environmental conditions affecting the reefs surrounding Piscadera Bay, which have undergone significant benthic cover transformations in recent decades (Sandin et al., 2022; De Bakker et al., 2016; Van Duyl, 1985). In-situ studies conducted around Piscadera Bay have demonstrated that turf algae and microalgae are more efficient than corals in taking up nutrients episodically released by plumes from the bay during rainfall events, providing these algae with a competitive advantage over corals (Den Haan et al., 2016; Vermeij et al., 2010). Our study also shows relatively high levels of elements such as Fe, Al, and Mn, which corroborates with the land-derived anthropogenic signatures found along the southwest coast of Curação (Van der Loosdrecht, submitted). Reefs close to land areas with increasing altered surface (i.e., the proportion of the onshore watershed that was occupied by humanmodified surfaces, including habitations, commercial developments, and roads) that can be associated with increased risk for urban runoff and pollution) showed higher loading of pollutants, and this correlation was enhanced with higher precepitation (Van de Loosdrecht, submitted). While XRF measurements are semi-quantitative and primarily reflect relative

https://doi.org/10.5194/egusphere-2025-4873 Preprint. Discussion started: 28 November 2025 © Author(s) 2025. CC BY 4.0 License.



655

656657

658 659

660

661 662

663

664

665

666

667

668 669

670

671

672

673674

675

676

677

678

679680

681

682

683 684



abundances, they are useful to indicate terrestrial runoff. In elevated concentrations, this material can be harmful to corals and promote growth of cyanobacteria and turf algae (Kelly, 2013; Esslemont, 1999). Turf algae, which can rapidly colonize newly available substratum, have become dominant on many coral reefs worldwide (Sandin et al., 2008b), further indicating ecosystem shifts in response to environmental changes. This pattern has also been seen over the past 40 years in the reefs of this study. Both the western and eastern reefs have experienced noticeable decrease in coral cover, now predominantly featuring turf algae and increased abundance of cyanobacterial mats, being more pronounced in the eastern reef, which is more directly subjected to bay-derived material (Sandin et al., 2022; De Bakker et al., 2016; Van Duyl, 1985). The western reef faces different conditions, characterized by trace-metal values that suggest alternative environmental pressures. While the semi-quantitative XRF measurements of Ni, Cu, Pb cannot be definitively classified as toxic, their presence indicates enhanced anthropogenic-related matter fluxes (Fernandez et al., 2007; Caballero-Gallardo et al., 2020). For example, Ni can limit calcium available for growth, affects respiration, and can reduce coral larvae settlement, coral reproduction and negatively affect growth and reproduction of other key reef organisms such as anemones or sea urchins (Méndez et al., 2021; Reichelt-Brushett and Hudspith, 2016; Reichelt-Brushett and Harrison, 2005; Nalley et al., 2021). Other elements such as Pb can also affect growth and photosynthesis of corals and macroalgaes (Baumann et al., 2009). Our findings align with studies suggesting that chronic exposure to certain pollutants may contribute to long-term reef degradation (Jackson et al., 2014). The rapid northwest surface current appears to play a crucial role in dispersing bay-derived materials away from nearshore areas, reducing residence time and potentially preventing the accumulation of high concentrations in localized zones. However, this same dispersal mechanism also facilitates the broader distribution of potential contaminants across the reef system. The contrasting hydrodynamic conditions between sites may explain observed differences in reef community composition, where the eastern reef-characterized by lower current velocities (Fig.2) and thus longer residence times-shows greater ecological degradation compared to the western reef (De Bakker et al., 2017; Sandin et al., 2022), which experiences higher current velocities (Fig.2) and more effective flushing by the main current





system. This differential exposure to terrestrial materials represents a critical factor in understanding current reef composition and predicting future development patterns (Fig. 9).

687

685 686

688

689 690

691

692

693 694

695

696

697

698 699

700

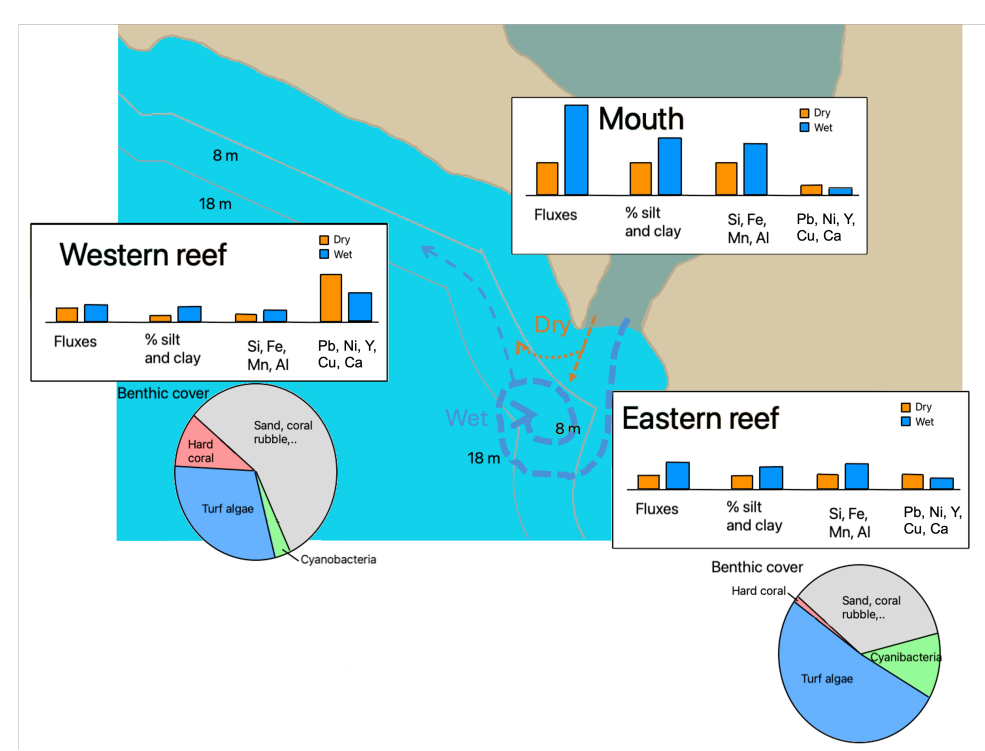


Figure 9. Summary of the spatial and seasonal variability in SPM characteristics in reefs nearby Piscadera Bay. (Graphical abstract)

5. Conclusions

This study highlights the spatial and seasonal dynamics of suspended particulate matter near Piscadera Bay, one of over 35 bays and water inlets along Curaçao's south coast that are subject to varying degrees of human impact. Seasonal differences show that dry-season SPM dynamics are controlled by localized factors (tides, resuspension, currents), while wet-season conditions are dominated by rainfall, wind, and enhanced hydrodynamics.

Coral reefs near bay mouths are particularly influenced by bay-derived inputs during wetseason runoff, with strengthening west-to-east correlations highlighting the role of bay-ocean exchange in transport processes. The eastern reef experiences prolonged exposure to





704705

706707

708

709

710

terrestrial material due to proximity and slower dispersal, potentially intensifying ecological stress, while the western reef benefits from rapid material dispersal.

The threat to reefs stems from increased pollutant loads and persistent fine particles that reduce light availability and transport harmful elements. In sheltered areas, slower hydrodynamic exchange prolongs these effects, altering material quality and quantity reaching reefs with important implications for reef health and resilience. Future research should compare SPM characteristics across multiple bays and include ecotoxicological assays to identify elements posing the greatest risk—essential for informing targeted mitigation strategies and evidence-based coastal management.

Acknowledgements

711 This publication is part of the project "Land, Sea, and Society: Linking terrestrial pollutants and 712 inputs to nearshore coral reef growth to identify novel conservation options for the Dutch Caribbean (SEALINK)" with project number NWOCA.2019.003 of the research program 713 714 "Caribbean Research: a Multidisciplinary Approach" which is (partly) financed by the Dutch 715 Research Council (NWO). We heartly thank the project leader Mark Vermeij for facilitating our 716 work at CARMABI. We thank Vesna Bertoncelj for helping processing the current data collected with the ADCP. We heartly thank Petra Visser for her advise. We greatly acknowledge 717 718 the team of CARMABI that helped sampling. We also want to thank Jeroen Kooijman for his 719 hard work and expert abilities in the XRF analysis. Finally, we gratefully thank Fay Diederiks and Julia Piaskowy for their help during fieldwork. 720

721 **Data**

724

- 722 The data supporting this study are openly available and can be accessed via the DOI:
- 723 https://dataportal.nioz.nl/doi/10.25850/nioz/7b.b.2j

Author Contributions

Virginia Sánchez Barranco: conceptualization, sampling, laboratory analysis, statistical analysis, and writing the first draft. Nienke C.J. van de Loosdrecht: conceptualization, sampling, laboratory analysis, and contribution to the final manuscript. Furu Mienis, Jasper M. de Goeij, and Lennart de Nooijer: conceptualization, funding acquisition, and contribution





- 729 to the final manuscript. Rick Hennekam, Gert-Jan Reichart, and Jan-Berend Stuut: contribution
- 730 to the final manuscript.

731 Competing Interests

732 The authors declare no competing interests.

References

- 734 Anthony, K. R.: Coral suspension feeding on fine particulate matter, Journal of Experimental
- 735 Marine Biology and Ecology, 232, 85-106, 1999.
- 736 Anthony, K. R. and Fabricius, K. E.: Shifting roles of heterotrophy and autotrophy in coral
- 737 energetics under varying turbidity, Journal of experimental marine biology and ecology, 252,
- 738 221-253, 2000.
- 739 Anthony, K. R., Kline, D. I., Diaz-Pulido, G., Dove, S., and Hoegh-Guldberg, O.: Ocean
- 740 acidification causes bleaching and productivity loss in coral reef builders, Proceedings of the
- 741 National Academy of Sciences, 105, 17442-17446, 2008.
- 742 Aronson, R. B., Bruno, J. F., Precht, W. F., Glynn, P. W., Harvell, C. D., Kaufman, L., Rogers, C. S.,
- 743 Shinn, E. A., and Valentine, J. F.: Causes of coral reef degradation, Science, 302, 1502-1504,
- 744 2003.
- 745 Bak, R. P.: Coral reefs and their zonation in Netherlands Antilles: modern and ancient reefs,
- 746 1977
- 747 Baumann, H. A., Morrison, L., and Stengel, D. B.: Metal accumulation and toxicity measured by
- 748 PAM—chlorophyll fluorescence in seven species of marine macroalgae, Ecotoxicology and
- 749 Environmental Safety, 72, 1063-1075, 2009.
- 750 Bergamaschi, B. A., Tsamakis, E., Keil, R. G., Eglinton, T. I., Montluçon, D. B., and Hedges, J. I.:
- 751 The effect of grain size and surface area on organic matter, lignin and carbohydrate
- 752 concentration, and molecular compositions in Peru Margin sediments, Geochimica et
- 753 Cosmochimica Acta, 61, 1247-1260, 1997.
- 754 Berry, K. L., Seemann, J., Dellwig, O., Struck, U., Wild, C., and Leinfelder, R. R.: Sources and
- 755 spatial distribution of heavy metals in scleractinian coral tissues and sediments from the Bocas
- 756 del Toro Archipelago, Panama, Environmental monitoring and assessment, 185, 9089-9099,
- 757 2013.
- 758 Bertoncelj, V., Mienis, F., Stocchi, P., and van Sebille, E.: Flow patterns, hotspots, and
- 759 connectivity of land-derived substances at the sea surface of Curação in the southern
- 760 Caribbean, Ocean Science, 21, 945-964, 2025.
- 761 Bertrand, S., Tjallingii, R., Kylander, M. E., Wilhelm, B., Roberts, S. J., Arnaud, F., Brown, E., and
- 762 Bindler, R.: Inorganic geochemistry of lake sediments: A review of analytical techniques and
- 763 guidelines for data interpretation, Earth-Science Reviews, 249, 104639, 2024.
- 764 Bhuyan, M. S., Jenzri, M., and Adikari, D.: Impacts of sedimentation on coral health and reef
- 765 ecosystems: A comprehensive review, Marine Pollution Bulletin, 221, 118480, 2025.
- Bothner, M. H., Reynolds, R. L., Casso, M. A., Storlazzi, C. D., and Field, M. E.: Quantity,
- 767 composition, and source of sediment collected in sediment traps along the fringing coral reef
- off Molokai, Hawaii, Marine Pollution Bulletin, 52, 1034-1047, 2006.
- 769 Burke, L. and Maidens, J.: Reefs at Risk in the Caribbean, 2004.
- 770 Burke, L., Reytar, K., Spalding, M., and Perry, A.: Reefs at risk revisited, Washington, DC: World
- 771 Resources Institute (WRI)2011.
- 772 Caballero-Gallardo, K., Alcala-Orozco, M., Barraza-Quiroz, D., De la Rosa, J., and Olivero-Verbel,
- 773 J.: Environmental risks associated with trace elements in sediments from Cartagena Bay, an
- industrialized site at the Caribbean, Chemosphere, 242, 125173, 2020.





- 775 Cuttler, M. V., Lowe, R. J., Falter, J. L., and Buscombe, D.: Estimating the settling velocity of
- 776 bioclastic sediment using common grain-size analysis techniques, Sedimentology, 64, 987-
- 777 1004, 2017.
- 778 D'Sa, E. J. and Ko, D. S.: Short-term influences on suspended particulate matter distribution in
- the northern Gulf of Mexico: Satellite and model observations, Sensors, 8, 4249-4264, 2008.
- 780 De Bakker, D. M., Meesters, E. H., Bak, R. P., Nieuwland, G., and Van Duyl, F. C.: Long-term shifts
- 781 in coral communities on shallow to deep reef slopes of Curação and Bonaire: are there any
- 782 winners?, Frontiers in Marine Science, 3, 247, 2016.
- 783 De Bakker, D. M., Van Duyl, F. C., Bak, R. P., Nugues, M. M., Nieuwland, G., and Meesters, E. H.:
- 40 Years of benthic community change on the Caribbean reefs of Curação and Bonaire: the rise
- of slimy cyanobacterial mats, Coral Reefs, 36, 355-367, 2017.
- 786 De Carlo, E. H., Hoover, D. J., Young, C. W., Hoover, R. S., and Mackenzie, F. T.: Impact of storm
- 787 runoff from tropical watersheds on coastal water quality and productivity, Applied
- 788 Geochemistry, 22, 1777-1797, 2007.
- 789 de Jong, C., van Os, I., Sepúlveda-Rodríguez, G., de Baat, M. L., and Schoepf, V.: High-resolution
- 790 temporal assessment of physicochemical variability and water quality in tropical semi-enclosed
- bays and coral reefs, Science of the Total Environment, 968, 178810, 2025.
- 792 Debrot, A., Kuenen, M., and Dekker, K.: Recent declines in the coral fauna of the Spaanse Water,
- 793 Curação, Netherlands Antilles, Bulletin of marine science, 63, 571-580, 1998.
- 794 Den Haan, J., Huisman, J., Brocke, H. J., Goehlich, H., Latijnhouwers, K. R., Van Heeringen, S.,
- 795 Honcoop, S. A., Bleyenberg, T. E., Schouten, S., and Cerli, C.: Nitrogen and phosphorus uptake
- 796 rates of different species from a coral reef community after a nutrient pulse, Scientific reports,
- 797 6, 28821, 2016.
- 798 Dutra, L., Kikuchi, R., and Leão, Z.: Effects of sediment accumulation on reef corals from
- 799 Abrolhos, Bahia, Brazil, Journal of Coastal Research, 633-638, 2006.
- 800 Dutra, L., Haywood, M. D., Singh, S. S., Piovano, S., Ferreira, M., Johnson, J. E., Veitayaki, J.,
- 801 Kininmonth, S. J., and Morris, C. W.: Effects of climate change on corals relevant to the Pacific
- 802 Islands, Pacific marine climate change report card, 132-158, 2018.
- 803 Erftemeijer, P. L., Riegl, B., Hoeksema, B. W., and Todd, P. A.: Environmental impacts of dredging
- and other sediment disturbances on corals: a review, Marine pollution bulletin, 64, 1737-1765,
- 805 2012
- 806 Esslemont, G.: Heavy metals in corals from Heron Island and Darwin harbour, Australia, Marine
- 807 Pollution Bulletin, 38, 1051-1054, 1999.
- 808 Fabricius, K. E.: Effects of terrestrial runoff on the ecology of corals and coral reefs: review and
- 809 synthesis, Marine pollution bulletin, 50, 125-146, 2005.
- 810 Fabricius, K. E. and Dommisse, M.: Depletion of suspended particulate matter over coastal reef
- 811 communities dominated by zooxanthellate soft corals, Marine Ecology Progress Series, 196,
- 812 157-167, 2000.
- 813 Fernandez, A., Singh, A., and Jaffé, R.: A literature review on trace metals and organic
- 814 compounds of anthropogenic origin in the Wider Caribbean Region, Marine Pollution Bulletin,
- 815 54, 1681-1691, 2007.
- 816 Gardner, W. D., Richardson, M. J., and Mishonov, A. V.: Global assessment of benthic nepheloid
- 817 layers and linkage with upper ocean dynamics, Earth and Planetary Science Letters, 482, 126-
- 818 134, 2018.
- 819 Gorgula, S. K. and Connell, S. D.: Expansive covers of turf-forming algae on human-dominated
- 820 coast: the relative effects of increasing nutrient and sediment loads, Marine Biology, 145, 613-
- 821 619, 2004.
- 822 Govers, L. L., Lamers, L. P., Bouma, T. J., de Brouwer, J. H., and van Katwijk, M. M.:
- 823 Eutrophication threatens Caribbean seagrasses–An example from Curação and Bonaire, Marine
- 824 pollution bulletin, 89, 481-486, 2014.





- 825 Guzmán, H. M. and Jiménez, C. E.: Contamination of coral reefs by heavy metals along the
- 826 Caribbean coast of Central America (Costa Rica and Panama), Marine Pollution Bulletin, 24,
- 827 554-561, 1992.
- 828 Heiskanen, A.-S. and Tallberg, P.: Sedimentation and particulate nutrient dynamics along a
- 829 coastal gradient from a fjord-like bay to the open sea, Biological, Physical and Geochemical
- 830 Features of Enclosed and Semi-enclosed Marine Systems: Proceedings of the Joint BMB 15 and
- 831 ECSA 27 Symposium, 9–13 June 1997, Åland Islands, Finland, 127-140,
- 832 Hodgson, G.: Sediment and the settlement of larvae of the reef coral Pocillopora damicornis,
- 833 Coral Reefs, 9, 41-43, 1990.
- 834 Hofker, J.: The foraminifera of Piscadera Bay, Curacao, Studies on the Fauna of Curacao and
- 835 other Caribbean Islands, 35, 1-62, 1971.
- 836 Ismail, M., Kimura, T., Suzuki, Y., and Tsuchiya, M.: Seasonal and spatial variations of total mass
- 837 flux around coral reefs in the southern Ryukyus, Japan, Journal of oceanography, 61, 631-644,
- 838 2005
- 839 Jackson, J., Donovan, M., Cramer, K., and Lam, V.: Status and trends of Caribbean coral reefs:
- 840 1970-2012, Gland, Switzerland: Global Coral Reef Monitoring Network; International ...2014.
- 841 Jouon, A., Ouillon, S., Douillet, P., Lefebvre, J. P., Fernandez, J. M., Mari, X., and Froidefond, J.-M.:
- 842 Spatio-temporal variability in suspended particulate matter concentration and the role of
- aggregation on size distribution in a coral reef lagoon, Marine Geology, 256, 36-48, 2008.
- 844 Kelly, L. E. W.: Coral reef microbes: the influences of benthic primary producers, nutrient
- availability, and anthropogenic stressors on community structure and metabolism, University of
- 846 California, San Diego2013.
- 847 Korte, L. F., Brummer, G.-J. A., Van Der Does, M., Guerreiro, C. V., Hennekam, R., Van Hateren, J.
- 848 A., Jong, D., Munday, C. I., Schouten, S., and Stuut, J.-B. W.: Downward particle fluxes of
- 849 biogenic matter and Saharan dust across the equatorial North Atlantic, Atmospheric Chemistry
- 850 and Physics, 17, 6023-6040, 2017.
- 851 Lakhan, V., Cabana, K., and LaValle, P.: Relationship between grain size and heavy metals in
- 852 sediments from beaches along the coast of Guyana, Journal of Coastal Research, 600-608,
- 853 2003
- 854 Larson, R. A., Brooks, G. R., Devine, B., Schwing, P. T., Holmes, C. W., Jilbert, T., and Reichart,
- 855 G.-J.: Elemental signature of terrigenous sediment runoff as recorded in coastal salt ponds: US
- Virgin Islands, Applied Geochemistry, 63, 573-585, 2015.
- 857 Li, X.-b., Huang, H., Lian, J.-s., Liu, S., Huang, L.-m., and Yang, J.-h.: Spatial and temporal
- 858 variations in sediment accumulation and their impacts on coral communities in the Sanya Coral
- 859 Reef Reserve, Hainan, China, Deep Sea Research Part II: Topical Studies in Oceanography, 96,
- 860 88-96, 2013.
- 861 Lobo, E. A., Heinrich, C. G., Schuch, M., Wetzel, C. E., and Ector, L.: Diatoms as bioindicators in
- 862 rivers, River algae, 245-271, 2016.
- 863 Malarkey, J., Baas, J. H., Hope, J. A., Aspden, R. J., Parsons, D. R., Peakall, J., Paterson, D. M.,
- 864 Schindler, R. J., Ye, L., and Lichtman, I. D.: The pervasive role of biological cohesion in bedform
- development, Nature communications, 6, 6257, 2015.
- 866 McCAVE, I.: Vertical flux of particles in the ocean, Deep Sea Research and Oceanographic
- 867 Abstracts, 491-502,
- 868 Méndez, S., Ruepert, C., Mena, F., and Cortés, J.: Accumulation of heavy metals (Cd, Cr, Cu, Mn,
- 869 Pb, Ni, Zn) in sediments, macroalgae (Cryptonemia crenulata) and sponge (Cinachyrella
- 870 kuekenthali) of a coral reef in Moín, Limon, Costa Rica: An ecotoxicological approach, Marine
- 871 Pollution Bulletin, 173, 113159, 2021.
- 872 Publications and Reports:
- 873 https://www.meteo.cw/publications_reports.php?Lang=Eng&St=TNCC, last access: 7 July
- 874 2025.





- 875 Nalley, E. M., Tuttle, L. J., Barkman, A. L., Conklin, E. E., Wulstein, D. M., Richmond, R. H., and
- 876 Donahue, M. J.: Water quality thresholds for coastal contaminant impacts on corals: A
- 877 systematic review and meta-analysis, Science of the Total Environment, 794, 148632, 2021.
- 878 Ng, M. S., Teo, A., and Todd, P. A.: Sediment trap height affects mass, particle size, and
- 879 biogeochemical composition of material collected in an equatorial coral reef, Marine Pollution
- 880 Bulletin, 183, 114086, 2022.
- 881 Nizou, J., Hanebuth, T. J., and Vogt, C.: Deciphering signals of late Holocene fluvial and aeolian
- 882 supply from a shelf sediment depocentre off Senegal (north-west Africa), Journal of Quaternary
- 883 Science, 26, 411-421, 2011.
- 884 Palmer, A. J. and Abbott, W. H.: Diatoms as indicators of sea-level change, in: Sea-level
- 885 Research: a Manual for the Collection and Evaluation of Data, Springer, 457-487, 1986.
- 886 Prochnow, D., Engelhardt, C., and Bungartz, H.: Dynamics of settling velocity distribution of
- 887 suspended particulate matter during sedimen-tation processes in rivers, WIT Transactions on
- 888 Ecology and the Environment, 33, 1970.
- 889 Ramos-Scharrón, C. E. and MacDonald, L. H.: Measurement and prediction of sediment
- 890 production from unpaved roads, St John, US Virgin Islands, Earth Surface Processes and
- 891 Landforms: The Journal of the British Geomorphological Research Group, 30, 1283-1304, 2005.
- 892 Reichelt-Brushett, A. and Hudspith, M.: The effects of metals of emerging concern on the
- 893 fertilization success of gametes of the tropical scleractinian coral Platygyra daedalea,
- 894 Chemosphere, 150, 398-406, 2016.
- 895 Reichelt-Brushett, A. J. and Harrison, P. L.: The effect of selected trace metals on the fertilization
- 896 success of several scleractinian coral species, Coral reefs, 24, 524-534, 2005.
- 897 Restrepo, J. C., Ortíz, J. C., Pierini, J., Schrottke, K., Maza, M., Otero, L., and Aguirre, J.:
- 898 Freshwater discharge into the Caribbean Sea from the rivers of Northwestern South America
- 899 (Colombia): Magnitude, variability and recent changes, Journal of Hydrology, 509, 266-281,
- 900 2014
- 901 Restrepo, J. D., Park, E., Aquino, S., and Latrubesse, E. M.: Coral reefs chronically exposed to
- 902 river sediment plumes in the southwestern Caribbean: Rosario Islands, Colombia, Science of
- 903 the Total Environment, 553, 316-329, 2016.
- 904 Rijsberman, F. and Westmacott, S.: Costeffectiveness analysis of coral reef management and
- 905 protection: A case study of Curacao, Integrated coastal zone management of coral reefs:
- 906 Decision support modeling. The International Bank for Reconstruction and Development, The
- 907 World Bank, Washington DC, USA, 49-66, 2000.
- 908 Ringuet, S. and Mackenzie, F. T.: Controls on nutrient and phytoplankton dynamics during
- 909 normal flow and storm runoff conditions, southern Kaneohe Bay, Hawaii, Estuaries, 28, 327-
- 910 337, 2005.
- 911 Risk, M. J.: Assessing the effects of sediments and nutrients on coral reefs, Current Opinion in
- 912 Environmental Sustainability, 7, 108-117, 2014.
- 913 Rogers, C. S.: Responses of coral reefs and reef organisms to sedimentation, Marine ecology
- 914 progress series. Oldendorf, 62, 185-202, 1990.
- 915 Rogers, C. S. and Ramos-Scharrón, C. E.: Assessing effects of sediment delivery to coral reefs: A
- 916 Caribbean watershed perspective, Frontiers in Marine Science, 8, 773968, 2022.
- 917 Salomons, W. and Förstner, U.: Metals in the Hydrocycle, Springer Science & Business
- 918 Media2012.
- 919 Sánchez Baranco, V., Schellenberg, L., Mienis, F., Brussaard, C., Haas, A., and de Nooijer, L.:
- 920 Seasonal changes in bay water column properties and their influence on the distribution of
- 921 dissolved and particulate substances along the south coast of Curação (Caribbean Sea),
- 922 Marine Pollution Bulletin, 212, 117545, 10.25850/nioz7b.b.0h, 2025.
- 923 Sánchez Barranco, V., Schellenberg, L., Mienis, F., Brussaard, C. P., Haas, A. F., and de Nooijer,
- 924 L. J.: Seasonal Changes in Bay Water Column Properties and Their Influence on the Distribution





- 925 of Dissolved and Particulate Substances Along the South Coast of Curação (Caribbean Sea),
- 926 Marine pollution bulletin, 10.25850/nioz7b.b.0h, 2025.
- 927 Sandin, S. A., Sampayo, E. M., and Vermeij, M. J.: Coral reef fish and benthic community
- 928 structure of Bonaire and Curação, Netherlands Antilles, Caribbean Journal of Science, 44, 137-
- 929 144, 2008a.
- 930 Sandin, S. A., Alcantar, E., Clark, R., de León, R., Dilrosun, F., Edwards, C. B., Estep, A. J.,
- 931 Eynaud, Y., French, B. J., and Fox, M. D.: Benthic assemblages are more predictable than fish
- 932 assemblages at an island scale, Coral reefs, 41, 1031-1043, 2022.
- 933 Sandin, S. A., Smith, J. E., DeMartini, E. E., Dinsdale, E. A., Donner, S. D., Friedlander, A. M.,
- 934 Konotchick, T., Malay, M., Maragos, J. E., and Obura, D.: Baselines and degradation of coral reefs
- 935 in the Northern Line Islands, PloS one, 3, e1548, 2008b.
- 936 Storlazzi, C. D., Field, M. E., and Bothner, M. H.: The use (and misuse) of sediment traps in coral
- 937 reef environments: theory, observations, and suggested protocols, Coral Reefs, 30, 23-38, 2011.
- 938 Storlazzi, C. D., Norris, B. K., and Rosenberger, K. J.: The influence of grain size, grain color, and
- 939 suspended-sediment concentration on light attenuation: Why fine-grained terrestrial sediment
- is bad for coral reef ecosystems, Coral Reefs, 34, 967-975, 2015.
- 941 Toro, P., Ibarra-gutierrez, K., Bernal, C., and Díaz, L.: Accumulation Rates Using the 210Pb
- 942 Dating Method in a Sediment Core of the Cispatá Bay, a Marine Protected Area in the
- 943 Southwestern Colombian Caribbean, Geology, Earth & Marine Sciences, 3, 1-5, 2021.
- 944 Tuttle, L. J. and Donahue, M. J.: Effects of sediment exposure on corals: a systematic review of
- 945 experimental studies, Environmental Evidence, 11, 4, 2022.
- 946 Van Der Does, M., Korte, L. F., Munday, C. I., Brummer, G.-J. A., and Stuut, J.-B. W.: Particle size
- 947 traces modern Saharan dust transport and deposition across the equatorial North Atlantic,
- 948 Atmospheric Chemistry and Physics, 16, 13697-13710, 2016.
- 949 Van Duyl, F. C.: Atlas of the Living Reefs of Cura «; ao and Bonaire (Netherlands Antilles),
- 950 Foundation for Scientific Research in Surinam and the Netherlands Antilles, 117, 1985.
- 951 Vega Thurber, R. L., Burkepile, D. E., Fuchs, C., Shantz, A. A., McMinds, R., and Zaneveld, J. R.:
- 952 Chronic nutrient enrichment increases prevalence and severity of coral disease and bleaching,
- 953 Global change biology, 20, 544-554, 2014.
- 954 Vermeij, M. J., van Moorselaar, I., Engelhard, S., Hörnlein, C., Vonk, S. M., and Visser, P. M.: The
- 955 effects of nutrient enrichment and herbivore abundance on the ability of turf algae to overgrow
- 956 coral in the Caribbean, PloS one, 5, e14312, 2010.
- 957 Wagenaar Hummelinck, P.: Marine localities, Studies on the Fauna of Curação and other
- 958 Caribbean Islands, 51, 1-68, 1977.
- 959 Weber, M., Lott, C., and Fabricius, K.: Sedimentation stress in a scleractinian coral exposed to
- 960 terrestrial and marine sediments with contrasting physical, organic and geochemical
- properties, Journal of experimental marine biology and ecology, 336, 18-32, 2006.
- 962 Weber, M., De Beer, D., Lott, C., Polerecky, L., Kohls, K., Abed, R. M., Ferdelman, T. G., and
- 963 Fabricius, K. E.: Mechanisms of damage to corals exposed to sedimentation, Proceedings of the
- 964 National Academy of Sciences, 109, E1558-E1567, 2012.
- 965 Weltje, G. J. and Tjallingii, R.: Calibration of XRF core scanners for quantitative geochemical
- 966 logging of sediment cores: Theory and application, Earth and Planetary Science Letters, 274,
- 967 423-438, 2008.
- 968 Wit, M. R., van Egmond, J.-L., Kruijssen, T. P., Bense, V. F., and van Breukelen, B. M.:
- 969 Hydrogeochemical signatures and human impact: A comprehensive analysis of groundwater
- 970 quality on the semi-arid island of Curação, Journal of Hydrology: Regional Studies, 60, 102555,
- 971 2025.
- 972 Zhang, J., Zhou, F., Chen, C., Sun, X., Shi, Y., Zhao, H., and Chen, F.: Spatial distribution and
- 973 correlation characteristics of heavy metals in the seawater, suspended particulate matter and
- 974 sediments in Zhanjiang Bay, China, PLoS One, 13, e0201414, 2018.